Effect of cannabidiol on cytokine-induced killer cells in multiple myeloma and pancreatic cancer

Doctoral thesis

to obtain a doctorate (PhD)

from the Faculty of Medicine

of the University of Bonn

Francesca Garofano

from Partinico, Italy

2022

Written with authorization of

the Faculty of Medicine of the University of Bonn

First reviewer: Prof. Dr. Ingo Schmidt-Wolf

Second reviewer: Prof. Dr. Hinrich Abken

Day of oral examination: 29/08/2022

From the Department of Integrated Oncology

Director: Prof. Dr. Ingo Schmidt-Wolf

Table of Contents

List of abbreviations

7-AAD	7-Aminoactinomycin D
AF488	AlexaFluor-488
AMP	3',5'-cyclic adenosine monophosphate
APC	Allophycocyanin
ATF-4	Activating Transcription Factor 4
BV	Brilliant violet
CB	Cannabinoid Receptor
CBD	Cannabidiol
CCK-8	Cell counting kit-8
CD	Cluster of Differentiation
CFSE	Carboxyfluorescein succinimidyl ester
CIK cells	Cytokine-induced killer cells
CNR	Cannabinoid receptor gene
CREB	cAMP response element-binding protein
DAP10	DNAX-activating protein 10
DAPI	4',6-diamidino-2-phenylindole
DMSO	Dimethyl sulfoxide
DNA	Deoxyribonucleic acid
dNTPs	Deoxyucleotide Triphosphate
DPBS	Dulbecco's Buffered Saline
DSMZ	German Collection of Microorganisms and Cell Cultures
ECS	Endocannabinoid System
ERK	Extracellular signal-regulated kinases
FACS	Fluorescent-activated cell sorting
FITC	Fluorescein isothiocyanate

GF	Growth factor
GPCR	G-protein coupled receptor
GPR55	G protein-coupled receptor 55
HEK	Human Embryonic Kidney
IFN	Interferon
IL	Interleukin
JAK/STAT	Janus Kinase and Signal Transducer and Activator of Transcription
LDH	Lactate Dehydrogenase
LFA-3	Lymphocyte Function associated antigen-3
MAM	Meprin, A-5 protein, and receptor protein-tyrosine phosphatase Mu
MAPK	Mitogen-activated protein kinase
MHC	Major histocompatibility Complex
MM	Multiple Myeloma
NCAM1	Neural cell adhesion molecule or CD56
NCS	Newborn Calf Serum
NF-kB	Nuclear Factor-kB
NK cells	Natural killer cells
NKG2D	Natural Killer Group 2 member D
NKT cells	Natural killer T cells
NRP	Neuropilin
P/S	Penicillin and Streptomycin
PB	Pacific blue
PBMC	Peripheral blood mononuclear cell
PC	Pancreatic cancer
PCs	Plasma cells
PE	R-Phycoerythrin
PFA	Paraformaldehyde
PPAR	Peroxisome proliferator-activated receptor

PPIA	Peptidylprolyl isomerase A
qRT-PCR	Quantitative Real Time Polymerase Chain Reaction
RBC	Red blood cell
RNA	Ribonucleic acid
RT	Room temperature
SEMA	Semaphorin
SQSTM1	Sequestosome1
SSC	Side scatter
TGF	Transforming growth factor
Th	T helper
THC	Tetrahydrocannabinol
TNF	Tumor Necrosis Factor
TRB3	Tribbles homolog 3
Treg cells	Regulatory T cells
TRPV	Transient Receptor Potential Vanilloid
VEGF	Vascular Endothelial Growth Factor
WGA	Wheat germ agglutinin

1. Abstract

Background/Aim: Cytokine-induced killer cells (CIKs) are a heterogeneous population of polyclonal T lymphocytes showing a potent anti-tumor activity. Cannabinoids have been recently used for the treatment of cancer. In this study, CIK cells were tested for cannabinoid receptor CB2 expression and downstream signaling. They were also analyzed for neuropiilin (NRP) proteins expression which have been proven to play an important role in cancer. Moreover, we investigated whether inducing CIK cells with cannabidiol (CBD) can enhance their cytotoxicity primarily in pancreatic cancer and myeloma cells. Materials and Methods: CIK cells were analyzed by using flow cytometry and quantitative real-time polymerase chain reaction for CB2 and Neuropilins expression in distinct cell populations. Using multiple methods (flow cytometry, immunohistochemistry, laser cell microscopy, cytotoxicity based in vitro assays), we addressed the CBD modulation along with CIK cells. Results: Flow cytometry analysis revealed remarkable high levels of CB2 expression in distinct cell populations of CIK cells on days 7 and 14 of *ex vivo* expansion compared to peripheral blood mononuclear PBMC cells. IL-2 modulates primarily the expression of the CB2 receptor on CIK cells. CBD can have a protective role for CIK cells, but when used during *ex vivo* expansion of CIK cells inhibits the growth of the NKT population. Downstream signaling phospho-p38 protein of CB2 was not detected in CIK cells, neither pancreatic cancer via flow cytometry. P-CREB was instead detected in CIK cells stimulated with pure cannabidiol, showing a difference within the different donors. Confocal microscopy experiments showed co-localization of p62 autophagosomal protein and CB2 receptors in CIK cells as well as pancreatic cancer cells. CIK cells were analyzed at different time points and the presence at low levels of NRP2, but not NRP1, was shown for CIK cells. CBD exerts an inhibition of CIK cytotoxic function against multiple myeloma (MM) and pancreatic cancer (PC) cells at high concentrations. Conclusions: A low dose of non-psychoactive CBD is sufficient to stimulate the cytotoxic function of CIK cells primarily in pancreatic and myeloma cells and may help to increase the therapeutic response. Recognizing NRP2 in CIK cells might help to improve CIK cell cytotoxicity.

2. Introduction and aims with references

The identification of endogenous compounds that bind to cannabinoid receptors gave rise to the concept of the endocannabinoid system (ECS) (Devane W.A. et al. 1992). It is an ubiquitous lipid signaling system which has important regulatory functions and is evolutionarily conserved from plants to mammals. The ECS, which includes the cannabinoid receptors, endocannabinoids, and their metabolizing enzymes, has been considered as a pharmacological target for the treatment of human diseases (Pertwee, R.G. 2009). Preparations from the plant *Cannabis sativa* (marijuana) have been widely used for centuries medicinally playing a role in the modulation of neurological and immunological functions. Cannabinoids produced by the Cannabis plant, called phytocannabinoids, have potential health applications and are known to exert palliative effects in cancer patients like the inhibition of chemotherapy-induced nausea and vomiting (Mortimer T.L. et al. 2019). Two major phytocannabinoids, (-)delta9-tetrahydrocannabinol (THC) and cannabidiol (CBD) are the most researched compounds and bind to cannabinoid receptors. They have been used for the treatment of cancer also as antitumor drugs based on their potential antitumor activity (Guzmán, M. 2003). In the mid 1960s to the early 1970s they were isolated cannabinoids from *Cannabis sativa* preparations including the identification of the main psychoactive constituent THC (Gaoni, Y. and Mechoulam, R. 1971). CBD is of particular interest since is not psychoactive but has significant relaxing, anti-inflammatory, pain-relieving and immunomodulatory properties. It took until 1990 for the first cannabinoid receptor to be identified and cloned the cannabinoid receptor CB1 (Matsuda L.A. et al., 1990). So far, the two endogenous cannabinoid-specific receptors CB1 and CB2 are the best characterized cannabinoids receptors in the ECS from mammalian tissues. They are members of the G-protein coupled receptors (GPCR) family and can signal through G-proteins of the $G_{i/0}$ type. In addition, other receptors, including the transient receptor potential vanilloid (TRPV1 and 2), G-protein coupled receptor GPR55 and the peroxisome proliferator-activated receptor gamma (PPARgamma) have been proposed to act as endocannabinoid receptors (Pertwee, R.G. at al. 2010). Whereas some

cannabinoids still interact with CB1 and CB2, they also interact with a large range of other targets including transporters, enzymes, cellular structures, membranes and ion channels (Watkins, A.R. 2019). The CB1 (encoded by the CNR1 gene) is expressed at high levels in the brain and at low levels in the non-hematopoietic system. CB2 instead (encoded by the CNR2 gene) is primarily expressed in cells and tissues of the immune system and is either not expressed or at very low levels in the non-hematopoietic cells in the brain (Howlett A.C. and Abood M.E. 2017). CBD is known to exert immunomodulatory effects through the activation of CB2. After engagement with an agonist ligand, CB2 is internalized and desensitized and an inverse agonist is able to reverse this process. CBD is an antagonist of CB1 and CB2 receptor agonists, and it also acts as an inverse agonist at CB1 and CB2 (Nichols, J.M. and Kaplan, B.L.F. 2020). Cytokine-induced killer cells (CIKs) are a heterogeneous population of polyclonal T lymphocytes obtained via ex vivo expansion of lymphocytes. They share phenotypic and functional characteristics with both, T cells and NK cells. Initially described in 1991 (Schmidt-Wolf I.G. et al. 1991), CIKs are efficiently expanded in vitro by incubation of peripheral blood mononuclear cell PBMCs with the timely addition of IFN-gamma on day 0 of culture, anti-CD3 antibody and IL-2 on the next day, followed by the subsequent addition of IL-2 during culture. Within the heterogeneous T cell population two main subpopulations can be distinguished, one coexpressing the CD3 and CD56 molecules (range: 40% to 80%), while the other presenting a CD3+ CD56- phenotype (range: 20% to 60%). It also comprises a small subpopulation (<10%) of CD3-CD56+ NK cells (Sangiolo, D. et al. 2008). The antitumor efficacy of CIKs has been reported to be associated with the CD3+CD56+ subset. The addition of IFN-gamma during generation of CIKs activates monocytes providing them with a contact-dependent factor CD58 (lymphocyte function associated antigen-3 LFA-3) and a soluble factor IL-12. These two factors are important for the expansion to CD56-positive T cells and the acquisition of T helper 1 phenotype of CIK cells (Lopez, R.D. 2000). CIKs are able to secrete TNF-alpha, IL-2 and IL-6 but are not able to secrete IL-4, IL-7 and IL-12. The complementary subsequent addition of anti-CD3 acts as a

mitogenic stimulus and high doses of IL-2 principally promote the expression of the natural killer group 2 member D (NKG2D) transmembrane adapter protein DAP10, which in turn is essential for cytolysis (Verneris, M.R. et al. 2004). The use of CIKs clinically is widely facilitated by the reproducibility and simplicity of the expansion protocol and their significant MHC-independent antitumor efficacy against a broad range of cancers. Compared to lymphokine-activated killer (LAK) cells which are induced by incubation with interleukin (IL) and tumor-infiltrating lymphocytes (TILs), CIK cells can be obtained more easily and reveal a higher tumor-specific cytotoxic activity. More extensive phenotypic analysis of expanded CD3+CD56+ cells showed that the most part are CD8+, but CD4+ cells can also be found to a lesser extent within CIKs cultures (Baker, J. et al. 2001). Other phenotypic characteristics of CIKs are the expression of CD5, CD11b and CD57 molecules and the Human Leukocyte Antigen-antigen D Related (HLA-DR) an MHC class II cell surface receptor. Unlike classic NKT cells, CIKs express a polyclonal TCR repertoire and are also independent from CD1 for their expansion. CIK cells have the potential to become key players in cancer treatment, therefore it is of importance to understand all genes and proteins involved in their mechanism of action. Neuropilins (NRPs) are 130-140kDa single pass transmembrane, non-tyrosine kinase surface glycoproteins expressed on the cell surface of cells of all vertebrate animals. Two homologous NRP isoforms are known, namely NRP1 and NRP2 (located on different genes), both originally discovered as neuronal adhesion molecules (Rossignol, M. et al. 2000). Many studies have revealed NRPs to be multifunctional proteins involved in a variety of biological processes, with NRP1 having a major role in immunity (Chuckran, C.A. 2020). NRP1 was the first to be described in 1987 and NRP2 was isolated later in 1997 (Chen, H. et al. 1997). They are composed by an extracellular domain, a transmembrane stretch, and a short intracellular tail. There are two complement binding factors in the extracellular part of NRP, two coagulation factor domains and one oligomerization domain. It also has a transmembrane and intracellular binding domain. The two most common molecules interacting with Neuropilins (NRP) are Class III Semaphorins (SEMA3) and Vascular Endothelial Growth factors (VEGF). The complement

binding domains and one of the coagulation binding domains are the site of SEMA binding, in contrast the coagulation factor domains are the sites for VEGF binding. SEMA3s is a family of molecules acting as repulsive or attractive signals for neuronal processes, in a complex with transmembrane receptors type-A plexins. NRPs are expressed in endothelial cells, where they interact with VEGF family members and some of their tyrosine kinase receptors enhancing their signaling cascade and promoting angiogenesis (Soker, S. et al. 1998). Previous studies have focused on the relation of Neuropilin expression on cancer cells finding a pattern that highlights the positive correlation between Neuropilin expression in tumour cells and the malignancy of such. Therefore, Neuropilin is becoming a protein of increased importance in regards to oncology research. Recently, it has also been demonstrated that NRP1 is a T cell memory checkpoint limiting long term antitumor immunity with the inhibition of $CD8^+$ T cell-mediated tumor immunosurveillance. The aims of the current study were, first, to verify the expression of the CB2 receptor on CIK cells at different times of *ex vivo* expansion, and the effect of CBD during CIK cells differentiation and on mature CIK cells. Second, to investigate the role of the different cytokines used for CIK cells differentiation on the expression of the CB2 receptor and the signals of CB2 in CIK cells. Third, to evaluate the effect of CBD on multiple myeloma and pancreatic cancer cells, including the effect of CBD on the cytotoxic activity of CIK cells against multiple myeloma and pancreatic cancer cells. Since Neuropilin has been proven to play a role in up-regulating signals involved with key pathways in the cell's cancerous lifespan, it was considered to be of interest to determine whether Neuropilin is present in CIK cells. Therefore, the fourth aim of this study was to experimentally determine the presence or absence of NRP-1 and NRP-2 in CIK cells.

References

A C Howlett, M E Abood. CB $_1$ and CB $_2$ Receptor Pharmacology. Adv Pharmacol 2017; 80:169-206.

A R Watkins. Cannabinoid interactions with ion channels and receptors. Channels (Austin) 2019; 13(1):162-167.

C A Chuckran, C Liu, T C Bruno, C J Workman, D A Vignali. Neuropilin-1: a checkpoint target with unique implications for cancer immunology and immunotherapy. J Immunother Cancer 2020; 8(2):e000967.

D Sangiolo, E Martinuzzi, M Todorovic, K Vitaggio, A Vallario, N Jordaney, F Carnevale-Schianca, A Capaldi, M Geuna, L Casorzo, et al. Alloreactivity and anti-tumor activity segregate within two distinct subsets of cytokine-induced killer (CIK) cells: Implications for their infusion across major HLA barriers. Int. Immunol. 2008, 20, 841–848.

H Chen, A Chédotal, Z He, C S Goodman, M Tessier-Lavigne. Neuropilin-2, a novel member of the neuropilin family, is a high affinity receptor for the semaphorins Sema E and Sema IV but not Sema III. Neuron 1997;19(3):547-59.

I G Schmidt-Wolf, R S Negrin, H P Kiem, K G Blume, I L Weissman. Use of a SCID mouse/human lymphoma model to evaluate cytokine-induced killer cells with potent antitumor activity. Exp. Med. 1991; 174, 139–149.

J Baker, M R Verneris, M Ito, J A Shizuru, R S Negrin. Expansion of cytolytic CD8(+) natural killer T cells with limited capacity for graft-versus-host disease induction due to interferon gamma production. Blood 2001; 97(10): 2923-2931.

J M Nichols, B L F Kaplan. Immune Responses Regulated by Cannabidiol. Cannabis Cannabinoid Res 2020; 5(1):12-31.

L A Matsuda, S J Lolait, M J Brownstein, A C Young, T I Bonner. Structure of a cannabinoid receptor and functional expression of the cloned cDNA. Nature 1990; 346(6284):561-4.

M Guzmán. Cannabinoids: potential anticancer agents. Nat Rev Cancer. 2003 Oct;3(10):745-55. doi: 10.1038/nrc1188.

M R Verneris, M Karami, J Baker, A Jayaswal, R S Negrin. Role of NKG2D signaling in the cytotoxicity of activated and expanded CD8+T cells. Blood 2004, 103, 3065–3072.

M Rossignol, M L Gagnon, M Klagsbrun. Genomic organization of human neuropilin-1 and neuropilin-2 genes: Identification and distribution of splice variants and soluble isoforms. Genomics 2000; 70, 211–222.

R D Lopez, E K Waller, P H Lu, R S Negrin. CD58/LFA-3 and IL-12 provided by activated monocytes are critical in the in vitro expansion of CD56+ T cells. Cancer Immunol. Immunother. 2000; 49, 629–640.

R G Pertwee, A C Howlett, M E Abood, S P H Alexander, V Di Marzo, M R Elphick, P J Greasley, H S Hansen, G Kunos, K Mackie, R Mechoulam, R A Ross. International Union of Basic and Clinical Pharmacology. LXXIX. Cannabinoid receptors and their ligands: beyond CB_1 and CB_2. Pharmacol Rev 2010; 62(4):588-631.

R G Pertwee. Emerging strategies for exploiting cannabinoid receptor agonists as medicines. Br J Pharmacol 2009; 156(3):397-411.

S Soker, S Takashima, H Q Miao, G Neufeld, M Klagsbrun. Neuropilin-1 is expressed by endothelial and tumor cells as an isoform-specific receptor for vascular endothelial growth factor. Cell 1998, 92, 735–745.

T L Mortimer, T Mabin, A M Engelbrecht. Cannabinoids: the lows and the highs of chemotherapy-induced nausea and vomiting. Future Oncol. 2019;15(9):1035-1049.

W A Devane, L Hanus, A Breuer, R G Pertwee, L A Stevenson, G Griffin, D Gibson, A Mandelbaum, A Etinger, R Mechoulam. Isolation and structure of a brain constituent that binds to the cannabinoid receptor. Science 1992; 258(5090):1946-9.

Y Gaoni, R Mechoulam. The isolation and structure of delta-1-tetrahydrocannabinol and other neutral cannabinoids from hashish. J Am Chem Soc 1971; 93(1):217-24.

3. Publications

3.1 Publication 1: High Expression of Cannabinoid Receptor 2 on Cytokine-Induced Killer Cells and Multiple Myeloma Cells

Article

High Expression of Cannabinoid Receptor 2 on Cytokine-Induced Killer Cells and Multiple Myeloma Cells

Francesca Garofano and Ingo G. H. Schmidt-Wolf *

Department of Integrated Oncology, Center for Integrated Oncology (CIO), University Hospital Bonn, 53127 Bonn, Germany; Francesca.Garofano@ukbonn.de
* Correspondence: ingo.schmidt-wolf@ukbonn.de; Tel.: +49-228-28717050; Fax: +49-228-28717065

check for updates

Abstract: Multiple myeloma (MM) is characterized by aberrant bone marrow plasma cell (PC) proliferation and is one of the most common hematological malignancies. The potential effect of cannabinoids on the immune system and hematological malignancies has been poorly characterized. Cannabidiol (CBD) may be used to treat various diseases. CBD is known to exert immunomodulatory effects through the activation of cannabinoid receptor 2 (CB2), which is expressed in high levels in the hematopoietic system. Cytokine-induced killer (CIK) cells are a heterogeneous population of polyclonal T lymphocytes obtained via ex vivo sequential incubation of peripheral blood mononuclear cells (PBMCs) with interferon-γ (IFN-γ), anti CD3 monoclonal antibody, and IL-2. They are characterized by the expression of CD3+ and CD56+, which are surface markers common to T lymphocytes and natural killer (NK) cells. CIK cells are mainly used in hematological patients who suffer relapse after allogeneic transplantation. Here, we investigated their antitumor effect in combination with pure cannabidiol in KMS-12 MM cells by lactate dehydrogenase LDH cytotoxicity assay, CCK-8 assay, and flow cytometry analysis. The surface and intracellular CB2 expressions on CIK cells and on KMS-12 and U-266 MM cell lines were also detected by flow cytometry. Our findings confirm that the CB2 receptor is highly expressed on CIK cells as well as on MM cells. CBD was able to decrease the viability of tumor cells and can have a protective role for CIK cells. It also inhibits the cytotoxic activity of CIKs against MM at high concentrations, so in view of a clinical perspective, it has to be considered that the lower concentration of 1 μM can be used in combination with CIK cells. Further studies will be required to address the mechanism of CBD modulation of CIK cells in more detail.

Keywords: cannabidiol; adoptive cellular immunotherapy; multiple myeloma; cytokine-induced killer cells; endocannabinoid system

1. Introduction

The human endocannabinoid system (ECS), which includes the cannabinoid receptors, endocannabinoids, and their metabolizing enzymes, has been considered as a pharmacological target for the treatment of various cancer types including multiple myeloma. Two major cannabinoids extracted from *Cannabis sativa* plant, called phytocannabinoids, (-)delta9-tetrahydrocannabinol (THC) [1] and cannabidiol (CBD) [2] which bind to cannabinoid receptors, are the most researched compounds and have been recently used for the treatment of cancer not only for their palliative effects like the treatment of pain and inhibition of vomiting associated with chemotherapy but also as antitumor drugs based on their potential antitumor activity. The best studied two endogenous cannabinoid receptors are cannabinoid receptor CB1 and CB2. They are members of the G-protein coupled receptors

(GPCR) family and can signal through G-proteins of the G $_{i/0}$ type [3]. The CB1 (encoded by the CNR1 gene) is expressed at high levels in the brain and at low levels in the hematopoietic system. Instead, the CB2 [4] (encoded by the CNR2 gene) is predominantly expressed in cells and tissues of the immune system and at low levels in the non-hematopoietic cells in the brain. The gene for CB2 receptor is located on chromosome 1p36 in humans and contains a single coding exon which is encoding for a 360-amino-acid-long single polypeptide chain. This comprises seven transmembrane alpha-helices with an extracellular glycosylated N-terminus and an intracellular C-terminus which is involved in signal transduction [5]. After engagement with an agonist ligand, CB2 is internalized and desensitized and an inverse agonist is able to reverse this process. CBD is an antagonist of CB1 and CB2 receptor agonists [6], and it also acts as an inverse agonist at CB1 and CB2. CBD can also interact with other molecular targets like vanilloid receptors (e.g., the transient receptor potential vanilloid type-1 and 2 TRPV1-2) [7], G protein-coupled receptor 55 (GPR55) [8], and peroxisome proliferator-activated receptor gamma (PPARgamma) [9]. It is of particular interest since it is not psychoactive but has significant relaxing, anti-inflammatory, pain-relieving, and immunomodulatory properties [10,11]. Current research supports the concept that CB2 is a promising therapeutic target for immune modulation. Although both hematopoietic and immune systems express high levels of CB2, the effect of cannabinoids on the immune system and hematological malignancies are poorly characterized. CB2 is active constitutively only on specific cells populations [12] and is expressed in high levels in B-cells which are precursors of plasma cells (PCs). Multiple myeloma (MM) is a PC malignancy and is one of the most common hematological malignancies. It is characterized by aberrant bone marrow PCs proliferation with excessive monoclonal protein production. It has been demonstrated that cannabinoids can induce a selective apoptosis in MM cell lines and PCs of MM patients which was mediated by caspase activation, mainly caspase-2, without harming normal cells and that blockage of the CB2 inhibited cannabinoid-induced apoptosis [13]. Morelli MB et al. reported that CBD strongly inhibited growth, arrested cell cycle progression, and induced MM cells death by regulating the ERK, AKT, and NF-κB pathways with major effects in TRPV2 positive cells [14,15]. It has been previously shown that CB2 signaling in unstimulated human immunocompetent primary leukocytes (peripheral blood mononuclear cells (PBMCs)) induced the secretion of IL-6 and IL-10 [16].

The use of immune therapy for the treatment of hematological malignancies is an effective obvious treatment for hematological malignancies, as they are more accessible to effector immune cells. Cytokine-induced killer (CIK) cells are easily developed ex vivo from PBMCs by adding the interferon-γ (IFN-γ), anti-CD3 mAb, IL-2, and IL-1β. CIK cells express the T-cell receptor CD3 as well as the natural killer cell receptor NKG2D (natural killer group 2 member D) that is thought to be responsible for the specific targeting of tumor cells [17,18]. The addition of IFN-γ during generation of CIK cells activates monocytes, providing them with a contact-dependent factor CD58 (lymphocyte function associated antigen-3 (LFA-3)) and a soluble factor IL-12. These two factors are important for the expansion to CD56-positive T cells and the acquisition of T helper 1 phenotype of CIK cells. The addition of anti-CD3 acts as a mitogenic stimulus and high doses of IL-2 principally promote the expression of the natural killer group 2 member D (NKG2D) transmembrane adapter protein DAP10, which is essential for cytolysis. CIK cells are able to secrete TNF-α, IL-2, and IL-6. The mechanism of CIK-associated tumor cytotoxicity has not been fully elucidated yet, including the efficiency of combining CIK and cannabidiol on tumor cells.

2. Results

2.1. CB2 is Detectable by Flow Cytometry on Days 7 and 14 in CIK Cells

Initial studies were performed to assess the differential expression of CB2 receptor in the main cell subsets of human CIK cells, i.e., CD3+ T lymphocytes (CD4+ and CD8+), CD56+ NK cells. We also analyzed CD20+ B cells and evaluated for both surface expression and intracellular CB2 expression by flow cytometry. The CIK cells were immunophenotyped at day 0 by flow cytometry. At day 0, CB2

expression was not detectable in any T lymphocytes subsets and B cells (Figure 1A). When CIK cells were activated at day 14, the CB2 expression was dramatically upregulated within the natural killer T (NKT) population CD3+CD56+T cells (Figure 1B) 98.1%. We also immunophenotyped CIK cells on day 7 in order to see at early stage the expression of CB2 receptor in the different populations (Figure 1C).
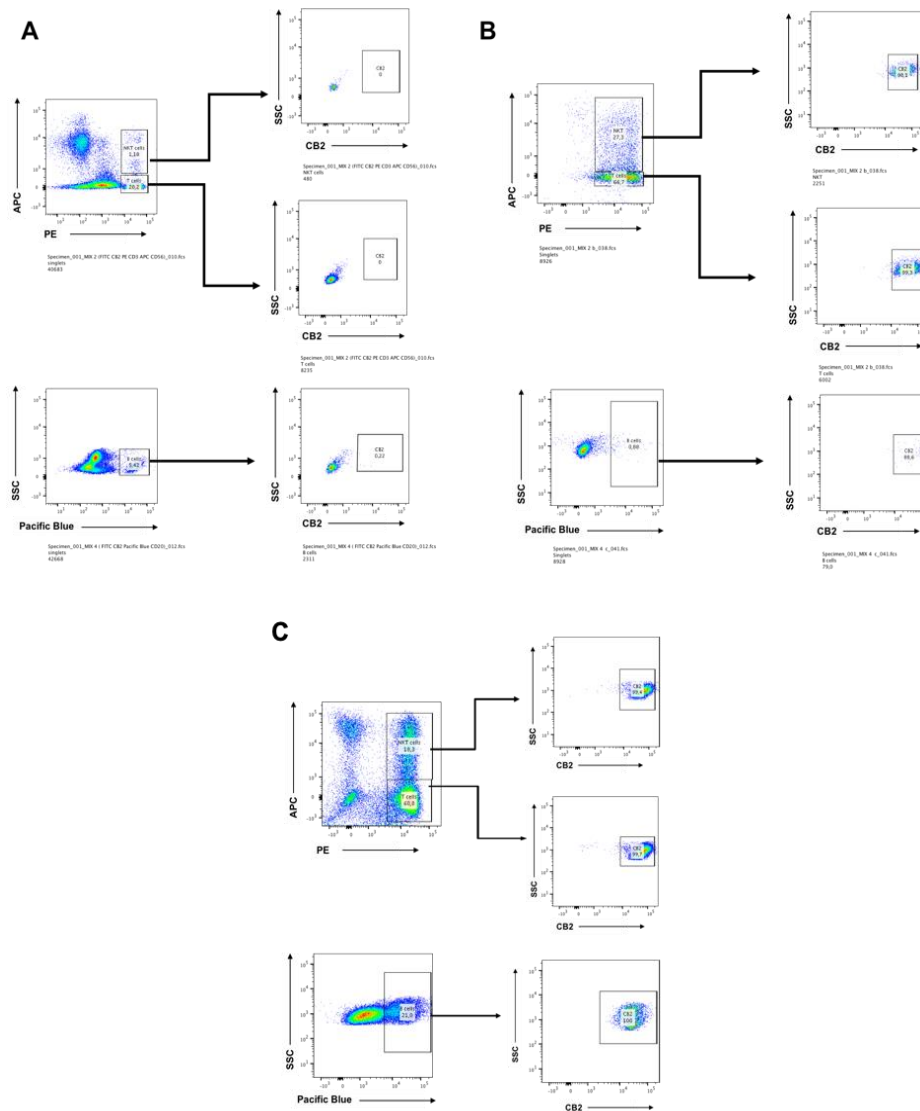
Figure 1. (**A**) The differential expression of CB2 receptor in the main cell subsets of human Cytokine-induced killer (CIK) cells, i.e., CD3+ T lymphocytes (CD4+ and CD8+), CD3+CD56+ NKT cells, and CD20+ B-cells. Both surface expression and intracellular CB2 expression were evaluated. The CIK cells were immunophenotyped at day 0 by flow cytometry. At day 0, CB2 expression was not detectable in any T lymphocytes subsets (CD3+ T lymphocytes 20.0%, CD3+CD56+ NKT 1.2%). Also, the B cells subset which was 5.4% did not express any CB2 receptor. (**B**) The CIK cells were immunophenotyped at day 14 by flow cytometry. Both surface expression and intracellular CB2 expression were evaluated. The T lymphocytes subsets were CD3+ T lymphocytes 66.7% and CD3+CD56+ NKT 27.3%. CB2 expression was dramatically upregulated within both CD3+ T lymphocytes (CD4+ and CD8+) 99.3% and the CD3+CD56+ NKT cells population 98.1%. The B cells subset was only the 0.9%. (**C**) The CIK cells were immunophenotyped on day 7 by flow cytometry. Both surface expression and intracellular CB2 expression were evaluated. The T lymphocytes subsets were CD3+ T lymphocytes 60.8% and CD3+CD56+ NKT 18.3%. CB2 expression was upregulated within both CD3+ T lymphocytes (CD4+ and CD8+) 99.7% and the CD3+CD56+ NKT cells population 99.4%. The B cells subset was the 21%, and all were positive for CB2 100%.

## 2.2. LDH Release of CIK Cells Significantly Decreases with CBD

The CCK8 assay was used as a direct measure of cell viability in CIKs exposed to various concentrations of CBD from 1 µM to 20 µM for 24 h. The results did not show any significant difference compared to the dimethyl sulfoxide (DMSO) control (Figure 2A). However, when the LDH assay was used as a direct measure of cytotoxicity in CIKs exposed to various concentrations of CBD from 1 µM to 20 µM for 24 h, the results showed that the LDH release of CIK cells was significantly decreased compared to the DMSO control (Figure 2B).
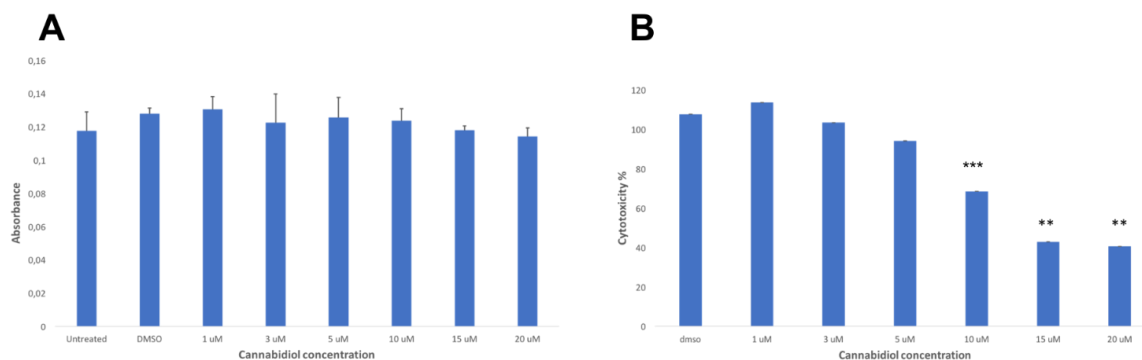
Figure 2. (**A**) The cell viability in CIKs exposed to various concentrations of Cannabidiol (CBD) for 24 h: The results of the CCK8 assay did not show any significant difference compared to the DMSO control ($p > 0.05$). (**B**) The cytotoxicity in CIKs exposed to various concentrations of CBD for 24 h: The results of the LDH assay showed a significant decrease of the LDH release at 10 µM ($p \leq 0.001$), 15 µM, and 20 µM ($p \leq 0.01$) compared to the DMSO control.

## 2.3. CB2 is Highly Expressed in Multiple Myeloma Cell Lines

Both surface and intracellular expressions of CB2 in KMS-12 PE and U-266 multiple myeloma cell lines were detected via flow cytometry analysis. The KMS-12 PE cell line which was established from the pleural effusion showed a very high level of CB2 receptor expression 98.4% (Figure 3A), and the U-266 cell line which was reported to produce IL-6 showed a very high level 98.8% (Figure 3B). This is in accordance with other studies showing the distribution of CB2 in the cells of the immune system where B lymphocytes express the highest amounts of CB2 followed in order by NK cells, macrophages, and T lymphocytes.
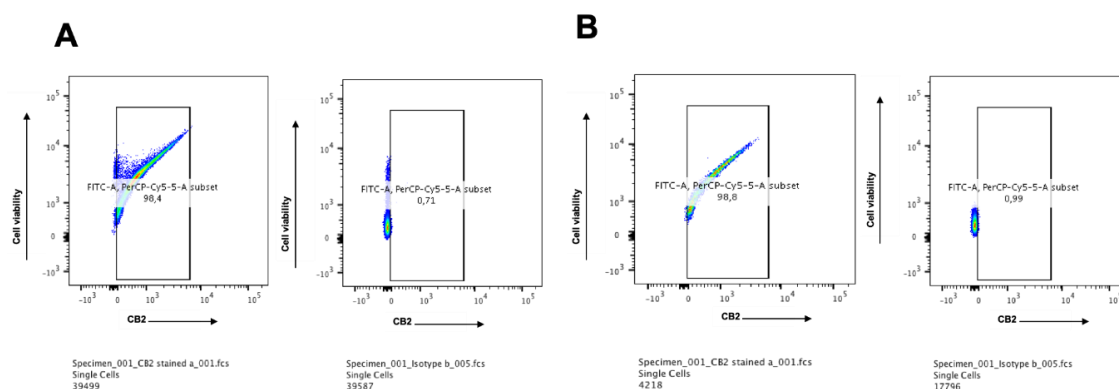
Figure 3. (**A**) Protein expression of the CB2 receptor on KMS-12 PE multiple myeloma cell line: Both intracellular and surface expressions of CB2 were detected by flow cytometry. The results showed that 98.4% of the cells express CB2 while the corresponding isotype control was 0.7%. (**B**) Protein expression of the CB2 receptor on U-266 multiple myeloma cell line: Both intracellular and surface expressions of CB2 were detected by flow cytometry. The results showed that 98.8% of the cells express CB2 while the corresponding isotype control was 1.0%.

## 2.4. CBD Significantly Increases the LDH Release of KMS Myeloma Cells at High Concentrations

The CCK8 assay was used as a direct measure of cell viability in KMS-12 PE cells exposed to various concentrations of CBD from 1 μM to 20 μM for 24 h. The results did not show any significant difference compared to the DMSO control (Figure 4A). However, when the LDH assay was used as a direct measure of cytotoxicity in KMS-12 PE cells exposed to various concentrations of CBD from 1 μM to 20 μM for 24 h, the results showed that the LDH release of KMS-12 PE cells was significantly increased compared to the DMSO control (Figure 4B).
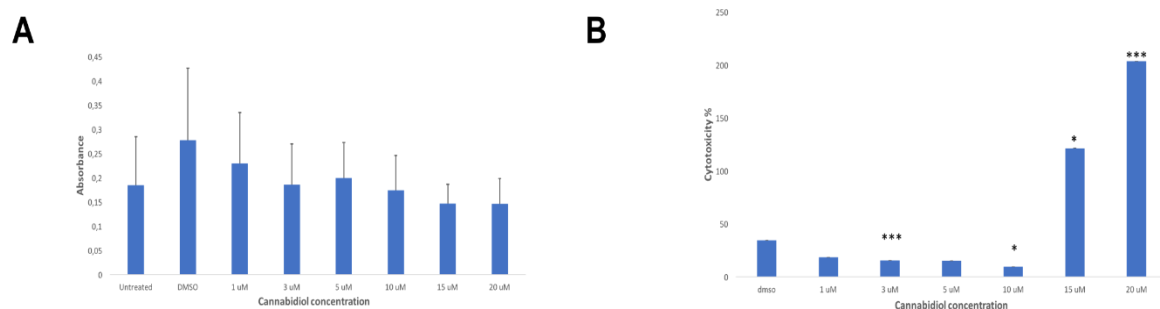
Figure 4. (**A**) The cell viability in KMS-12 PE cells exposed to various concentrations of CBD for 24 h: The results of the CCK8 assay did not show any significant difference compared to the DMSO control ($p > 0.5$). (**B**) The cytotoxicity in in KMS-12 PE cells exposed to various concentrations of CBD for 24 h: The results of the LDH assay showed a significant decrease of the LDH release at 3 μM ($p \leq 0.001$) and 10 μM ($p < 0.05$) compared to the DMSO control. However, the results showed a significant increase at 15 μM ($p < 0.05$) and 20 μM ($p \leq 0.001$) compared to the DMSO control.

2.5. CBD Significantly Decreases the Cytotoxicity of CIK Cells Against KMS Cells at High Concentrations

When finally the effector cells were co-cultured with the target cells (KMS-12 PE) with an E:T ratio 10:1 and exposed to various concentrations of CBD from 1 μM to 20 μM for 24 h, a concentration-dependent inhibition response was recorded via flow cytometry analysis (Figure 5A). Similar results were obtained when the LDH cytotoxicity experiment was used (Figure 5B). We also reported the absolute number of viable residual CIK cells (CD3+CD56+ NKT cells population) after treatment with CBD from 1 μM to 20 μM (Figure 5C). The results confirmed that CBD has a protective role for CIK cells at a concentration of 1 μM.
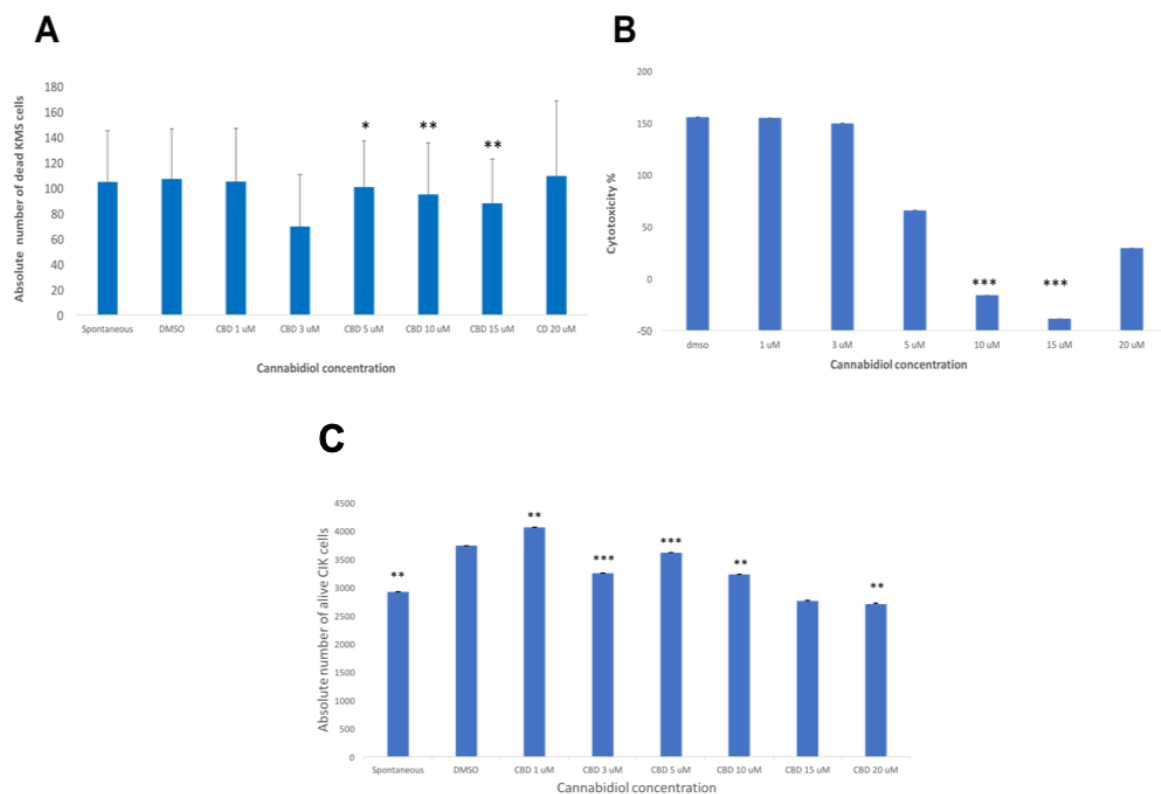
Figure 5. (**A**) The absolute number of dead KMS-12 PE cells was calculated for each sample condition of co-cultured CIKs and KMS-12 PE cells exposed to various concentrations of CBD for 24 h via flow cytometry analysis. The results showed a significant decrease of the absolute number of the dead KMS-12 PE cells at 5 μM ($p < 0.05$), 10 μM, and 15 μM ($p \leq 0.01$) compared to the DMSO control. (**B**) The cytotoxicity of the effector CIKs against target KMS-12 PE cells exposed to various concentrations of CBD for 24 h was analyzed via LDH assay. The results of the LDH assay showed a significant decrease of the LDH release at 10 μM and 15 μM ($p \leq 0.001$) compared to the DMSO control. (**C**) The absolute number of alive CIK cells (CD3+CD56+ NKT cells population) was calculated for each sample condition of co-cultured CIKs and KMS-12 PE cells exposed to various concentrations of CBD for 24 h via flow cytometry analysis. The results showed a significant decrease of the absolute number of the alive CIK cells compared to the DMSO control ($p \leq 0.01$) and a significant increase of the absolute number of the alive CIK cells at 1 μM ($p < 0.001$), 3 μM ($p \leq 0.001$), 5 μM ($p \leq 0.001$), and 10 μM ($p \leq 0.01$) compared to the DMSO control. There was a significant decrease at 20 μM ($p \leq 0.01$).

2.6. CBD Inhibits the Growth of NKT Cells

We performed some studies to assess the differential expression of NKG2D receptor in the main cell subsets of human CIK cells, i.e., CD3+ T lymphocytes (CD4+ and CD8+) and CD56+ NK cells for surface NKG2D expression by flow cytometry. CIK cells were differentiated either with DMSO alone, CBD 10 μM, or untreated. CIK cells were immunophenotyped at day 14 by flow cytometry. The results showed that CBD 10 μM was able to decrease the percentage of NKT cells compared to the untreated and DMSO control (Figure 6). However, the percentage of NKG2D-positive NKT cells did not change between them.
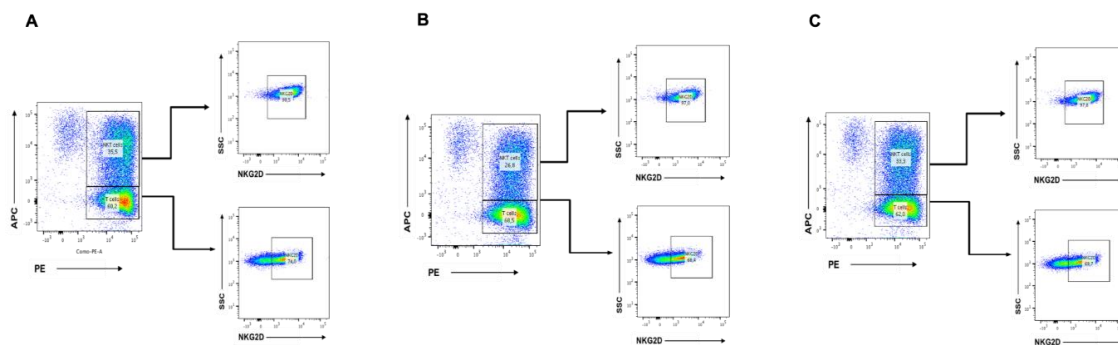
Figure 6. (A) The differential expression of the natural killer group 2 member D (NKG2D) receptor in the main cell subsets of human CIK cells, i.e., CD3+ T lymphocytes (CD4+ and CD8+) and CD3+CD56+ NKT cells: The surface NKG2D expression was evaluated. The CIK cells were immunophenotyped at day 14 by flow cytometry. In the untreated, both T lymphocytes subsets CD3+ T lymphocytes 60.2% and CD3+CD56+ NKT 35.5% showed high expressions of NKG2D receptor 74% and 98.5%, respectively. **(B)** In the untreated CBD 10 μM, both T lymphocytes subsets CD3+ T lymphocytes 68.5% and CD3+CD56+ NKT 26.8% showed high expressions of NKG2D receptor 68.4% and 97%, respectively. **(C)** In the DMSO control, both T lymphocytes subsets CD3+ T lymphocytes 62% and CD3+CD56+ NKT 33.3% showed high expressions of NKG2D receptor 69.7% and 97.8%, respectively.

3. Discussion

Endocannabinoids have been reported to affect immune function, and the cannabinoid receptor that, for the most part, is linked to the modulation of the immune responses is CB2. The factors and conditions that regulate CB2 expression are still poorly understood, and the signaling cascades are incomplete. Cannabinoids also have been reported to suppress a variety of activities of T lymphocytes in a mode that appears to be linked functionally to CB2. The results from a number of studies suggested that cannabinoids not only exert direct effects on immune cells but also elicit a shift in the cytokine expression profile from that which is pro-inflammatory (Th1) to one that is anti-inflammatory (Th2). Cytokine-induced killer (CIK) cells are an heterogenous T cell population capable of exerting a potent major histocompatibility complex (MHC)-unrestricted cytotoxicity against both hematologic and solid tumors but not hematopoietic precursors and normal tissues [19]. Within the heterogeneous T cell population, two main subpopulations can be distinguished, one coexpressing the CD3 and CD56 molecules (range: 40% to 80%) while the other presenting a CD3+ CD56- phenotype (range: 20% to 60%). It also comprises a small subpopulation (<10%) of CD3- CD56+ NK cells [20]. The antitumor efficacy of CIKs has been reported to be associated with the CD3+CD56+ subset that serves as the main effector cells combining T cell capability with NK cell function. It has been demonstrated that cannabinoids can induce a selective apoptosis in MM cell lines and PCs of MM patients which was mediated by caspase activation and that CIK cells were resistant to Fas-mediated apoptosis that could be induced by the expression of FasL on cancer cells.

Although the expression and function of CB1 and CB2 receptors has been widely studied in several immune cells, as yet, no studies have addressed the expression of CB2 on CIK cells. In the attempt to shed some light on the CIK cells of subsets that could express CB2, we performed polychromatic flow cytometry that allowed simultaneous interrogation of receptor expression in distinct cell populations. Such a multiparametric approach revealed remarkable high levels of CB2 expression in KSM-12 PE and U-266 cell lines in CIK cells on days 7 and 14. Here, we demonstrate that cannabinoid exerts an inhibition of CIK cytotoxic function against multiple myeloma (MM) cell line KMS-12 PE at high concentrations. Additionally, this is the first study reporting a detailed characterization of CB2 expression in human mature CIK cells and these two tumor cell lines by using flow cytometry directly.

The results of the LDH cytotoxicity assay showed that CBD can affect the viability of MM cells. These results confirm the antitumor potential of CBD against MM, which was already reported by

other studies based on the analysis of apoptosis. However, CBD can be protective regarding CIK cells since the LDH release was decreasing in a dose-dependent manner. In view of a clinical perspective, it has to be considered that the lower concentration of 1 μM could be used in the combination with CIK cells. Further studies will be required to address the mechanisms of the CIK cells whereby CB2 modulates interaction in more detail.

4. Materials and Methods

4.1. Generation of Cytokine-Induced Killer Cells

Peripheral blood mononuclear cells (PBMC) were isolated from blood samples of healthy donors after obtaining written informed consents, and isolation was carried out on the same day or kept overnight at 4 °C for use on the next day. Blood was mixed with Dulbecco's phosphate-buffered saline (DPBS; PAN BIOTECH, Aidenbach, Germany)-ethylenediaminetetracetic acid (EDTA; Life Technologies, PAA, Cölbe, Germany) (1:250) in a 50-mL falcon tube at a ratio of 1:1 and added to another falcon tube containing Lymphoprep density gradient medium (Pancoll) (PAN BIOTECH, Aidenbach, Germany) in order to perform a density gradient centrifugation. The collected PBMC were washed twice with DPBS-EDTA. Erythrocytes were lysed and washed away with red blood cell (RBC) lysis buffer (Biolegend, San Diego, CA, USA) and another DPBS-EDTA washing step. The cells obtained were counted and plated at a density of $1–2 \times x \; 10^6$ cells/mL in a T-175 flask containing 40 mL of culture medium RPMI 1640 (PAN BIOTECH, Aidenbach, Germany) supplemented with 10% newborn calf serum (NCS) (Sigma, St. Louis, MO, USA), 1% penicillin and streptomycin P/S (Gibco, Gaithersburg, MD, USA), and 1 M Hepes (PAN BIOTECH, Aidenbach, Germany). After 2 h, the flask was changed in order to eliminate the adherent cells and 20 μl of IFN-gamma (ImmunoTools GmbH, Friesoythe, Germany) was added ($2000 \; U \; \mu L^{-1}$). On the next day, 100 μL of IL-1β (ImmunoTools GmbH, Friesoythe, Germany) ($40 \; U \; \mu L^{-1}$), 2 μL of anti-CD3 antibody (eBioscience, Thermo Fisher Scientific, Inc. San Diego, CA, USA) (1 mg/mL), as well as 24 μL of IL-2 (ImmunoTools GmbH, Friesoythe, Germany) ($1000 \; U \; \mu L^{-1}$) were added to the cells. Every 3 days, half of the medium was exchanged and 600 U/ mL IL-2 were added. After day 14 of culture, the cells were considered mature CIK cells.

4.2. Cell Lines and Cell Culture

Multiple myeloma cell line KMS-12 PE and U-266 (obtained from Leibniz Institute DSMZ Deutsche Sammlung von Mikroorganismen und Zellkulturen) were cultured in RPMI 1640 (PAN BIOTECH, Aidenbach, Germany) supplemented with 10% newborn calf serum (NCS) (Sigma, St. Louis, MO, USA) and 1% penicillin and streptomycin P/S (Gibco, Gaithersburg, MD, USA) at 37 °C in a humidified atmosphere with 5% CO_2.

4.3. Cell Viability Analysis

Cell viability analysis was performed by a Cell Counting Kit-8 (CCK-8) assay. MM cell lines and CIK cells were exposed to different concentrations of pure cannabidiol (100%) (Santa Cruz Biotechnologie, Heidelberg, Germany) from 1 μM to 20 μM for 24 h at 37 °C. The effector cells (CIK cells) were co-cultured with target cells (KMS-12 PE) at effector and target (E:T) ratios of 10:1 and seeded into flat bottom 96-well plates. Next, 10 μL of CCK-8 reagent (Dojindo, Kumamoto, Japan) was added to the cells according to the manufacturer's instructions. They were incubated for 1 h in the incubator; then, the absorbance was measured at 450 nm using a microplate reader. All the experiments were performed in triplicates, and the results were normalized. This experiment was replicated three times with CIK cells from three different donors.

4.4. LDH Assay

A commercial Pierce™ LDH Cytotoxicity Assay Kit (ThermoFisher, Waltham, MA, USA) was used according to the manufacturer's instructions. MM cell lines and CIK cells were exposed to different concentrations of pure cannabidiol (Santa Cruz Biotechnologie, Heidelberg, Germany) from 1 μM to 20 μM for 24 h at 37 °C. The effector cells (CIK cells) were co-cultured with target cells (KMS-12 PE) at effector and target (E:T) ratios of 10:1 and seeded into 48-well plates. The absorption of the released LDH was then measured with a microplate reader at 490 nm and 680 nm. At the end of incubation, 25 μL of each sample was transferred to a 96-well flat bottom plate in different wells, and 25 μL of the reaction mixture was added to each well. To determine LDH activity, the 680 nm absorbance value is substracted from the 490 nm absorbance value. All experiments were performed in triplicates. Experiments were replicated three times with CIK cells from three different donors. In order to calculate % cytotoxicity, the following equation was applied to the corrected values:

$$\% \text{ citotoxicity } = \frac{\text{Experimental value} - \text{Effector Cells Spontaneous Control} - \text{Target Cells Spontaneous Control}}{\text{Target Cells Maximum Control} - \text{Target Cells Spontaneous Control}} \times 100$$

To calculate % cytotoxicity of CBD on CIK cells or tumor cells, the following equation was applied to the corrected values:

$$\% \text{ citotoxicity } = \frac{\text{Compound} - \text{treated LDH activity} - \text{Spontaneous LDH activity}}{\text{Maximum LDH activity} - \text{Spontaneous LDH activity}} \times 100$$

4.5. Fluorescence-Activated Cell Sorting (FACS) Analysis

The following antihuman antibodies were used to stain cell surface markers to establish the CIK phenotype: CD3-fluorescein isothiocyanate (FITC) (Biolegend, San Diego, CA, USA), CD56-phycoerythrin (PE) (Biolegend, San Diego, CA, USA), CD4-allophycocyanin (APC) (Biolegend), CD8-Brilliant Violet 421(BV421) (Biolegend, San Diego, CA, USA), CD3-phycoerythrin (PE) (Biolegend, San Diego, CA, USA), CD56-allophycocyanin (APC) (Biolegend, San Diego, CA, USA), CD20-Pacific Blue (Biolegend, San Diego, CA, USA), and FITC-NKG2D (Biolegend, San Diego, CA, USA). For surface and intracellular CB2 receptor staining, CIK cells and tumor cells were fixed and permeabilized with Invitrogen Intracelluar Fix & Perm set kit (ThermoFisher, Waltham, MA, USA) according to the manufacturer's instructions. The cells were stained with a FITC-conjugated antibody against CB2 (Cayman Chemical, Michigan, USA) and an anti-rabbit IgG FITC-conjugated anti-CB2 antibody (Cayman Chemical, Michigan, USA). Zombie Aqua™ Fixable Viability Kit (Biolegend, San Diego, CA, USA) permeant to cells with compromised membranes was used to stain the dead CIK cells and 7-Aminoactinomycin D (7-AAD) (Biolegend, San Diego, CA, USA) to stain the dead tumor cells. To assess the cytotoxicity of CIK cells in combination with pure cannabidiol (Santa Cruz Biotechnologie, Heidelberg, Germany) on multiple cell lines, the carboxyfluorescein succinimidyl ester (CFSE; ThermoFisher, Waltham, MA, USA)-labeled multiple myeloma cells were incubated along with Far Red (ThermoFisher, Waltham, MA, USA.)-labeled CIK cells in an E:T ratio of 10:1 and exposed to different concentrations of pure cannabidiol from 1 μM to 20 μM for 24 hours at 37 °C. Pure cannabidiol was first solved in DMSO and afterwards diluted within the corresponding RPMI medium (PAN BIOTECH, Aidenbach, Germany). The cell suspensions the were washed with DPBS (PAN BIOTECH, Aidenbach, Germany) twice. Finally, the dead cells were stained with Hoechst 33258 (Cayman Chemical, Michigan, USA) and Precision Count Beads™ (Biolegend, San Diego, CA, USA) were added.

Conflicts of Interest: The authors declare no conflict of interest.

References

1. Gaoni, Y.; Mechoulam, R. Isolation, structure and partial synthesis of an active constituent of Hashish. *J. Am. Chem. Soc.* **1964**, *86*, 1646–1647. [CrossRef]
2. Izzo, A.A.; Borrelli, F.; Capasso, R.; Di Marzo, V.; Mechoulam, R. Non-psychotropic plant cannabinoids: New therapeutic opportunities from an ancient herb. *Trends Pharmacol. Sci.* **2009**, *30*, 515–527. [PubMed]
3. Howlett, A.C.; Qualy, J.M.; Khachatrian, L.L. Involvement of Gi in the inhibition of adenylate cyclase by cannabimimetic drugs. *Mol. Pharmacol.* **1986**, *29*, 307–313. [PubMed]
4. Munro, S.; Thomas, K.L.; Abu-Shaar, M. Molecular characterization of a peripheral receptor for cannabinoids. *Nature* **1993**, *365*, 61–65. [CrossRef] [PubMed]
5. Bouaboula, M.; Dussossoy, D.; Casellas, P. Regulation of peripheral cannabinoid receptor CB2 phosphorylation by the inverse agonist SR144528. Implications for receptor biological responses. *J. Biol. Chem.* **1999**, *274*, 20397–20405. [PubMed]
6. Thomas, A.; Baillie, G.L.; Phillips, A.M.; Razdan, R.K.; Ross, R.A.; Pertwee, R.G. Cannabidiol displays unexpectedly high potency as an antagonist of CB1 and CB2 receptor agonists in vitro. *Br. J. Pharmacol.* **2007**, *150*, 613–623. [CrossRef] [PubMed]
7. Caterina, M.J.; Schumacher, M.A.; Tominaga, M.; Rosen, T.A.; Levine, J.D.; Julius, D. The capsaicin receptor: A heat-activated ion channel in the pain pathway. *Nature* **1997**, *389*, 816–824. [CrossRef] [PubMed]
8. Ryberg, E.; Larsson, N.; Sjögren, S.; Hjorth, S.; Hermansson, N.O.; Leonova, J.; Elebring, T.; Nilsson, K.; Drmota, T.; Greasley, P.J. The orphan receptor GPR55 is a novel cannabinoid receptor. *Br. J. Pharmacol.* **2007**, *152*, 1092–1101. [PubMed]
9. Ramer, R.; Heinemann, K.; Merkord, J.; Rohde, H.; Salamon, A.; Linnebacher, M.; Hinz, B. COX-2 and PPAR-gamma confer cannabidiol-induced apoptosis of human lung cancer cells. *Mol. Cancer Ther.* **2013**, *12*, 69–82. [CrossRef] [PubMed]
10. Mechoulam, R.; Peters, M.; Murillo-Rodriguez, E.; Hanus, L.O. Cannabidiol–recent advances. *Chem. Biodivers.* **2007**, *4*, 1678–1692. [CrossRef] [PubMed]
11. Velasco, G.; Sánchez, C.; Guzmán, M. Towards the use of cannabinoids as antitumour agents. *Nat. Rev. Cancer* **2012**, *12*, 436–444. [PubMed]
12. Galiegue, S.; Mary, S.; Marchand, J.; Dussossoy, D.; Carrière, D.; Carayon, P.; Bouaboula, M.; Shire, D.; Le Fur, G.; Casellas, P. Expression of central and peripheral cannabinoid receptors in human immune tissues and leukocyte subpopulations. *Eur. J. Biochem.* **1995**, *232*, 54–61. [CrossRef] [PubMed]
13. Barbado, M.V.; Medrano, M.; Caballero-Velázquez, T.; Álvarez-Laderas, I.; Sánchez-Abarca, L.I.; García-Guerrero, E.; Martín-Sánchez, J.; Rosado, I.V.; Piruat, J.I.; Gonzalez-Naranjo, P.; et al. Cannabinoid derivatives exert a potent anti-myeloma activity both in vitro and in vivo. *Int. J. Cancer* **2017**, *1*, 674–685. [CrossRef] [PubMed]
14. Morelli, M.B.; Offidani, M.; Alesiani, F.; Discepoli, G.; Liberati, S.; Olivieri, A.; Santoni, M.; Santoni, G.; Leoni, P.; Nabissi, M. The effects of cannabidiol and its synergism with bortezomib in multiple myeloma cell lines. A role for transient receptor potential vanilloid type-2. *Int. J. Cancer* **2014**, *134*, 2534–2546. [CrossRef] [PubMed]
15. Nabissi, M.; Morelli, M.B.; Offidani, M.; Amantini, C.; Gentili, S.; Soriani, A.; Cardinali, C.; Leoni, P.; Santoni, G. Cannabinoids synergize with carfilzomib, reducing multiple myeloma cells viability and migration. *Oncotarget* **2016**, *7*, 77543–77557. [PubMed]
16. Saroz, Y.; Kho, D.; Glass, M.; Graham, E.S.; Grimsey, N.L. Cannabinoid Receptor 2 (CB$_2$) Signals via G-alpha-s and Induces IL-6 and IL-10 Cytokine Secretion in Human Primary Leukocytes. *ACS Pharmacol. Transl. Sci.* **2019**, *2*, 414–428. [CrossRef] [PubMed]
17. Lu, P.H.; Negrin, R.S. A novel population of expanded human CD3+CD56+ cells derived from T cells with potent in vivo antitumor activity in mice with severe combined immunodeficiency. *J. Immunol.* **1994**, *153*, 1687–1696.

18. Sangiolo, D. Cytokine induced killer cells as promising immunotherapy for solid tumors. *J. Cancer* **2011**, *2*, 363–368. [PubMed]
19. Schmidt-Wolf, I.G.; Negrin, R.S.; Kiem, H.P.; Blume, K.G.; Weissman, I.L. Use of a SCID mouse/human lymphoma model to evaluate cytokine-induced killer cells with potent antitumor cell activity. *J. Exp. Med.* **1991**, *174*, 139–149. [CrossRef] [PubMed]
20. Schmidt-Wolf, I.G.; Lefterova, P.; Johnston, V.; Huhn, D.; Blume, K.G.; Negrin, R.S. Propagation of large numbers of T cells with natural killer cell markers. *Br. J. Haematol.* **1994**, *87*, 453–458. [CrossRef] [PubMed]

3.2 Publication 2: A Low Dose of Pure Cannabidiol Is Sufficient to Stimulate the Cytotoxic Function of CIK Cells without Exerting the Downstream Mediators in Pancreatic Cancer Cells

Article

A Low Dose of Pure Cannabidiol Is Sufficient to Stimulate the Cytotoxic Function of CIK Cells without Exerting the Downstream Mediators in Pancreatic Cancer Cells

Francesca Garofano [1], Amit Sharma [1,2], Hinrich Abken [3], Maria A. Gonzalez-Carmona [4] and Ingo G. H. Schmidt-Wolf [1,*]

1   Department of Integrated Oncology, Center for Integrated Oncology (CIO), University Hospital Bonn, 53127 Bonn, Germany; francesca.garofano@ukbonn.de (F.G.); amit.sharma@ukbonn.de (A.S.)
2   Department of Neurosurgery, University Hospital Bonn, 53127 Bonn, Germany
3   RCI Regensburg Center for Interventional Immunology, Department Genetic Immunotherapy, University Hospital Regensburg, 93053 Regensburg, Germany; hinrich.abken@ukr.de
4   Department of Internal Medicine I, University Hospital Bonn, 53127 Bonn, Germany; maria.gonzalez-carmona@ukbonn.de
*   Correspondence: ingo.schmidt-wolf@ukbonn.de; Tel.: +49-228-2871-7050; Fax: +49-228-2871-7065

Abstract: Despite numerous studies conducted over the past decade, the exact role of the cannabinoid system in cancer development remains unclear. Though research has focused on two cannabinoid receptors (CB1, CB2) activated by most cannabinoids, CB2 holds greater attention due to its expression in cells of the immune system. In particular, cytokine-induced killer cells (CIKs), which are pivotal cytotoxic immunological effector cells, express a high-level of CB2 receptors. Herein, we sought to investigate whether inducing CIK cells with cannabidiol can enhance their cytotoxicity and if there are any possible counter effects in its downstream cascade of phosphorylated p38 and CREB using a pancreatic ductal adenocarcinoma cell line (PANC-1). Our results showed that IL-2 modulates primarily the expression of the CB2 receptor on CIK cells used during ex vivo CIK expansion. The autophagosomal-associated scaffold protein p62 was found to co-localize with CB2 receptors in CIK cells and the PANC-1 cell line. CIK cells showed a low level of intracellular phospho-p38 and, when stimulated with cannabidiol (CBD), a donor specific variability in phospho-CREB. CBD significantly decreases the viability of PANC-1 cells presumably by increasing the cytotoxicity of CIK cells. Taken together, in our preclinical in vitro study, we propose that a low effective dose of CBD is sufficient to stimulate the cytotoxic function of CIK without exerting any associated mediator. Thus, the combinatorial approach of non-psychactive CBD and CIK cells appears to be safe and can be considered for a clinical perspective in pancreatic cancer.

Keywords: cytokine-induced killer cells; cannabidiol; pancreatic cancer

1. Introduction

Cancer is a heterogeneous disease where multiple overlapping molecular pathways are involved [1]. In fact, the combinatorial role of various inhibitors/compounds is constantly being explored along with several therapeutic approaches in order to overcome the impact of this disease. In this scenario, the pivotal role of cytokine-Induced killer (CIK) cells as a cellular antitumor therapy cannot be ignored. CIK cells share phenotypic and functional properties of both T cells and NK cells, and are easily expandable to test in culture. Moreover, CIK therapy has been proven effective and safe in the treatment of various cancers and recently celebrated 30 years of successful implementation [2]. To mention, CIK cells display encouraging synergistic effects when combined with cancer associated inhibitors/blockades [3,4]. Since cannabinoid receptors have been the subject of intensive cancer research [5,6], in particular, cannabinoid receptor 2 (CB2) holds greater attention due to its expression in cells of the immune system where CIK cells also play an

important role. To mention, recently, we have also shown that CIK cells express high levels of CB2 receptor compared to PBMCs [7].

Specifically, in pancreatic cancer (PC), where several clinical trials based on CIK cell therapy have yielded encouraging results [8,9], cannabinoids have also been reported to inhibit pancreatic cancer cell growth in vitro and in vivo through various mechanisms [10]. PC as a fatal illness is usually recognized late in the metastatic stage, primarily due to the anatomic localization of the pancreas and the nonspecific nature of the symptoms. Despite all clinical and molecular advances [11–13], PC still harbors a very poor prognosis and high mortality rate [14]; therefore, it is of prime interest to set up new strategies. Previously, synthetic cannabinoid derivatives have been shown to induce cell death in pancreatic MIA PaCa-2 cells via a receptor-independent mechanism [15]. Moreover, human PC cell lines and tumor biopsies have been shown to express higher levels of cannabinoid receptors compared to normal pancreatic tissue [16]. The same study also demonstrated that cannabinoids lead to apoptosis of pancreatic tumor cells via a CB2 receptor and de novo synthesized ceramide-dependent up-regulation of p8 and the endoplasmic reticulum stress–related genes ATF-4 and TRB3. Interestingly, the scaffold/phagosomal protein p62/SQSTM1 has recently been identified as part of the CB2 receptor interactome in transfected HEK293 cells [17]. Likewise, an independent interesting study demonstrated that CB2 induces the phosphorylation of p38 MAPKs, downstream CREB phosphorylation and induction of IL-6, IL-10 cytokine secretion in human primary leukocytes [18]. It is noteworthy that the exact mode of action of these cannabinoid receptors is unclear, despite being involved in immune system like CIK cells, their possible crosstalk and underlying mechanisms remain unexplored.

Considering this, herein, we sought to investigate whether inducing CIK cells with cannabidiol can enhance their cytotoxicity. While we focused primarily on PC in this study, we also used myeloma cells as a proof of concept. Using multiple methods (Flow cytometry, immunohistochemistry, laser cell microscopy, cytotoxicity based in vitro assays), we address the cannabidiol modulation along with CIK cells.

2. Materials and Methods

2.1. Generation of Cytokine-Induced Killer Cells

Peripheral blood mononuclear cells (PBMCs) were isolated from blood samples of healthy donors after obtaining the approval of the ethics committee of the University Hospital Bonn, including a signed informed consent from the volunteers. The isolation was carried out on the same day or kept overnight at 4 °C for further use on the next day. Briefly, the blood was mixed with Dulbecco's phosphate-buffered saline (DPBS; PAN BIOTECH, Aidenbach, Germany)-ethylenediaminetetracetic acid (EDTA; Life Technologies, PAA, Cölbe, Germany) (1:250) in a 50 mL falcon tube at a ratio of 1:1 and then transferred to another falcon tube containing Lymphoprep density gradient medium (Pancoll) (PAN BIOTECH, Aidenbach, Germany) in order to perform a gradient density centrifugation. The collected PBMC were washed twice with DPBS-EDTA. Erythrocytes were lysed and washed away with red blood cell (RBC) lysis buffer (Biolegend, San Diego, CA, USA) and subsequently washed with DPBS-EDTA. The cells obtained were then seeded at a density of $1–2 \times 10^6$ cells/mL in a T-175 flask containing 40 mL of culture medium RPMI 1640 (PAN BIOTECH, Aidenbach, Germany) supplemented with 10% newborn calf serum (NCS) (Sigma, St. Louis, MO, USA), 1% penicillin and streptomycin P/S (Gibco, Gaithersburg, MD, USA), and 1 M Hepes (PAN BIOTECH, Aidenbach, Germany). The generation of CIK cells was primed by adding 20 µL of IFN-γ (ImmunoTools GmbH, Friesoythe) (2000 U/µL) on day 0. On the next day, 100 µL of IL-1 (ImmunoTools GmbH, Friesoythe, Germany) (40 U/µL), 2 µL of anti-CD3 antibody (eBioscience, Thermo Fisher Scientific, Inc., San Diego, CA, USA) (1 mg/mL), as well as 24 µL of IL-2 (ImmunoTools GmbH, Friesoythe, Germany) (1000 U/µL) or IL-15 (40 ng/mL) (ImmunoTools GmbH, Friesoythe, Germany) were added into the cells. Every third day, half of the medium was exchanged and 600

U/mL IL-2 or IL-15 (40 ng/mL) were added. The CIK cells were expanded for 14 days ex vivo and used for co-culturing experiments.

2.2. Cell Line and Cell Culture

In the current study, we utilized two cell lines, one sourced from pancreatic cancer (Pancreatic ductal adenocarcinoma cell line: PANC-1) and another from multiple myeloma (U-266), both obtained from Leibniz Institute DSMZ Deutsche Sammlung von Mikroorganismen und Zellkulturen. Both cell lines were cultured in RPMI 1640 (PAN BIOTECH, Aidenbach, Germany) supplemented with 10% newborn calf serum (NCS) (Sigma, St. Louis, MO, USA) and 1% penicillin and streptomycin P/S (Gibco, Gaithersburg, MD, USA) at 37 °C in a humidified atmosphere with 5% CO_2.

2.3. Cytotoxicity Assay Based on CCK-8

After co-culture with CIK cells for 24 h, the cells' viability of PANC-1, U-266 tumor cell lines and CIK cells exposed to different concentrations (1–20 µM, at 37 °C) of pure cannabidiol (CBD 100%) (Santa Cruz Biotechnologie, Heidelberg, Germany) was determined by CCK-8 based method. Briefly, the effector cells (CIK cells) were co-cultured with target cells (PANC-1, U-266) at the effector to target (E:T) ratios of 10:1 and seeded into flat bottom 96-well plates. Next, 10 µL of CCK-8 reagent (Dojindo, Kumamoto, Japan) were added in each well, according to the manufacturer's instructions. After incubation for 1 h, the absorbance of each well was measured at 450 nm using a microplate reader. All the experiments were performed in triplicates. This particular experiment was replicated three times with CIK cells from three different donors.

2.4. LDH Assay

A commercial CyQUANT LDH Cytotoxicity Assay Kit (ThermoFisher, Waltham, MA, USA) was used, according to the manufacturer's instructions. Here again, PANC-1, U-266 cell lines and CIK cells were exposed to different concentrations (1–20 µM, 24 h at 37 °C) of pure cannabidiol (CBD) (Santa Cruz Biotechnologie, Heidelberg, Germany). The effector cells (CIK cells) were co-cultured with target cells (PANC-1, U-266) at the effector to target (E:T) ratios of 10:1 and seeded into 48-well plates. At the end of incubation, 25 µL of each sample were transferred to a 96-well flat bottom plate and 25 µL of the reaction mixture were added. The absorption of the released LDH was then measured using a microplate reader at 490 nm and 680 nm. To determine LDH activity, the 680 nm absorbance value was subtracted from the 490 nm absorbance value. All experiments were performed in triplicates and replicated three times with CIK cells from three different donors. To calculate the % cytotoxicity, the following equation was applied to the corrected values:

$$\%cytotox. = \frac{\text{Experimental value } - \text{ Effector Cells Spontaneous Control } - \text{ Target Cells Spontaneous Control}}{\text{Target Cells Maximum Control } - \text{ Target Cells Spontaneous Control}} \times 100$$

To calculate the % cytotoxicity of CBD on tumor cells, the following equation was applied to the corrected values:

$$\%cytotox. = \frac{\text{Compound} - \text{treated LDH activity } - \text{ Spontaneous LDH activty}}{\text{Maximum LDH activty } - \text{ Spontaneous LDH activty}} \times 100$$

2.5. Immunocytochemistry

PANC-1 and CIK cells were plated on poly-L-Lysine (Sigma, St. Louis, MO, USA) coated glass cover slips with their respective cell culture medium. After 2 h incubation at 37 °C, cells were washed with DPBS (PAN BIOTECH, Aidenbach, Germany) and stained with the lectin WGA conjugated with Texas red (1:200) (Thermo Fisher, Waltham, MA, USA). After washing, the cells were permeabilized with 4% PFA (Sigma, St. Louis, MO, USA) for 10 min at RT followed by an incubation with primary antibodies for CB2 (1:300)

(Abnova, Taipei, Taiwan) and p62 (1:300) (Sigma, St. Louis, MO, USA), for 20 min at RT in DPBS (PAN BIOTECH, Aidenbach, Germany). Next, secondary antibodies (1:2000) were incubated for 1 h at RT, and cells were then washed and mounted with DAPI (1:5000) (ThermoFisher, Waltham, MA, USA).

2.6. Imaging and 3D Reconstruction Modeling

Four colors confocal images were acquired from a confocal laser scan microscope (Leica TCS SP8). As excitation, four laser lines, 405, 488, 561, and 633 nm were primarily employed and, for the excitation and detection of the fluorescent signal, a 63xNA objective lens was used. The fluorescent signal was directed to a HyD after being spectrally separated. All the post-processing analysis and evaluation for images were performed using the software Imaris. A segmentation algorithm was used to isolate a structure of the CB2 co-localization with p62. Segmented images were than displayed and image snapshots were taken.

2.7. Fluorescence-Activated Cell Sorting (FACS) Analysis

The following antihuman antibodies were used to stain cell surface markers to establish the CIK phenotype: CD3-fluorescein isothiocyanate (FITC) (Biolegend, San Diego, CA, USA), CD56-phycoerythrin (PE) (Biolegend, San Diego, CA, USA), CD4-allophycocyanin (APC) (Biolegend), CD8-Brilliant Violet 421(BV421) (Biolegend, San Diego, CA, USA), CD3-phycoerythrin (PE) (Biolegend, San Diego, CA, USA), CD56-allophycocyanin (APC) (Biolegend, San Diego, CA, USA), and CD20-Pacific Blue (Biolegend, San Diego, CA, USA). For the surface and intracellular CB2 receptor staining, CIK cells and tumor cells were fixed and permeabilized with Invitrogen Intracelluar Fix & Perm set kit (ThermoFisher, Waltham, MA, USA), according to the manufacturer's instructions. The cells were then stained with a FITC-conjugated antibody against CB2 (Cayman Chemical, City, MI, USA) and anti-rabbit IgG FITC-conjugated anti-CB2 antibody (Cayman Chemical, City, MI, USA). For intracellular p-38 and p62 proteins staining, cells were stained with a PE-conjugated antibody against p-38 MAPKs (ThermoFisher, Waltham, MA, USA) and AlexaFluor488-conjugated antibody against p62/SQSTM1 (JSR Life Sciences, Sunnyvale, CA, USA). 7-Aminoactinomycin D (7-AAD) (Biolegend, San Diego, CA, USA) was used to stain the dead tumor cells. To assess the cytotoxicity of CIK cells in combination with pure cannabidiol (Santa Cruz Biotechnologie, Heidelberg, Germany) in cell lines, the carboxyfluorescein succinimidyl ester (CFSE; ThermoFisher, Waltham, MA, USA)-labeled multiple pancreatic and multiple myeloma cancer cells were incubated along with Far Red (ThermoFisher, Waltham, MA, USA.)-labeled CIK cells in an E:T ratio of 10:1 and exposed to different concentrations (1–20 μM, 24 h at 37 °C) of pure cannabidiol (CBD). Pure cannabidiol was first solved in DMSO and afterwards diluted within the corresponding RPMI medium (PAN BIOTECH, Aidenbach, Germany). The cell suspensions were washed with DPBS (PAN BIOTECH, Aidenbach, Germany) twice. Finally, the dead cells were stained with Hoechst 33258 (Cayman Chemical, City, MI, USA) and Precision Count Beads (Biolegend, San Diego, CA, USA) were added.

2.8. CREB Phosphorylation Assay (p-CREB)

CIK cells at 14 days of culture were pelleted by centrifugation for 5 min at 1500 rpm, resuspended in cell culture medium and seeded at 1×10^7 cells/mL (200 μL of cells per well) in 96-well tissue culture treated plates. Plates were incubated at 37 °C in a humidified atmosphere with 5% CO_2 for 2 h and incubated 30 min prior to adding of pure cannabidiol (CBD, 100%) (Santa Cruz Biotechnologie, Heidelberg, Germany) from 1 μM to 20 μM. At the end of the incubation, cells were lysed by the addition of lysis buffer on a plate shaker for 10 min at RT. p-CREB detection was performed using the AlphaLISA SureFire Ultra p-CREB (ser133) assay kit (PerkinElmer, Waltham, MA, USA). The signal was detected on a SpectraMax plate reader with AlphaLISA-compatible filters.

3. Results

3.1. IL-2 Primarily Determines the Expression of CB2 Receptor on CIK Cells

CIK cells were generated from the PBMCs of healthy volunteers and phenotypes of CD3$^+$CD56$^+$ (NKT), CD3$^+$CD56$^-$ (T cells) and CD3$^-$CD56$^+$ (NK) were confirmed to see both surface and intracellular CB2 expression. Primarily, we observed CD3$^+$CD56$^+$ (23.1%), CD3$^+$CD56$^-$ (52.5%), and CD3$^-$CD56$^+$ (21.0%) CIK cells without anti-CD3 antibody and CD3$^+$CD56$^+$ (18.5%), CD3$^+$CD56$^-$ (75.6%), and CD3$^-$CD56$^+$ (2.58%) cells tested in the absence of IFN-γ (Figure 1). In addition, 3.92% CD20$^+$ B cells without anti-CD3 antibody (Figure 1A) and 1.99% without IFN-γ were detected.

It is worth noting that the percentage of CB2-positive cells within these different subgroups did not differ significantly and remained completely positive. Of interest, when we used half of the amount of IL-2, the percentages of CD3$^+$CD56$^+$ (NKT), CD3$^+$CD56$^-$ (T cells) and CD3$^-$CD56$^+$ (NK) cells were 17.8%, 56.9%, and 14.0%, while in complete absence of IL-2, they were 30.4%, 67.7%, and 0.49%, respectively (Figure 1B). Importantly, the percentages of CB2 positive cells within CD3$^+$CD56$^+$ (59.0%), CD3$^+$CD56$^-$ (50.6%), and CD3$^-$CD56$^+$ (70.1%) decreased significantly in the complete absence of IL-2, while it remains entirely positive when only half of the amount of IL-2 was used. In addition, 55.3% CD20$^+$ B cells were detected with half of the amount and 2.72% by a complete lack of IL-2; however, the percentages of CB2 positive cells remain high in both conditions. We extended our analysis by testing IL-15 or no IL-1β in a similar experimental setup and observed CD3$^+$CD56$^+$ (8.02%), CD3$^+$CD56$^-$ (81.3%), and CD3$^-$CD56$^+$ (7.07%) CIK cells with IL-15 and CD3$^+$CD56$^+$ (30.04%), CD3$^+$CD56$^-$ (67.7%), and CD3$^-$CD56$^+$ (0.49%) cells in the absence of IL-1β (Figure 1C). In this case, 10.0% CD20$^+$ B cells were detected with IL-15 and 6.22% by a complete lack of IL-1β. Here again, the percentages of CB2 positive cells remain high in both conditions—thus indicating that IL-2 primarily determines the expression of the CB2 receptor on CIK cells.
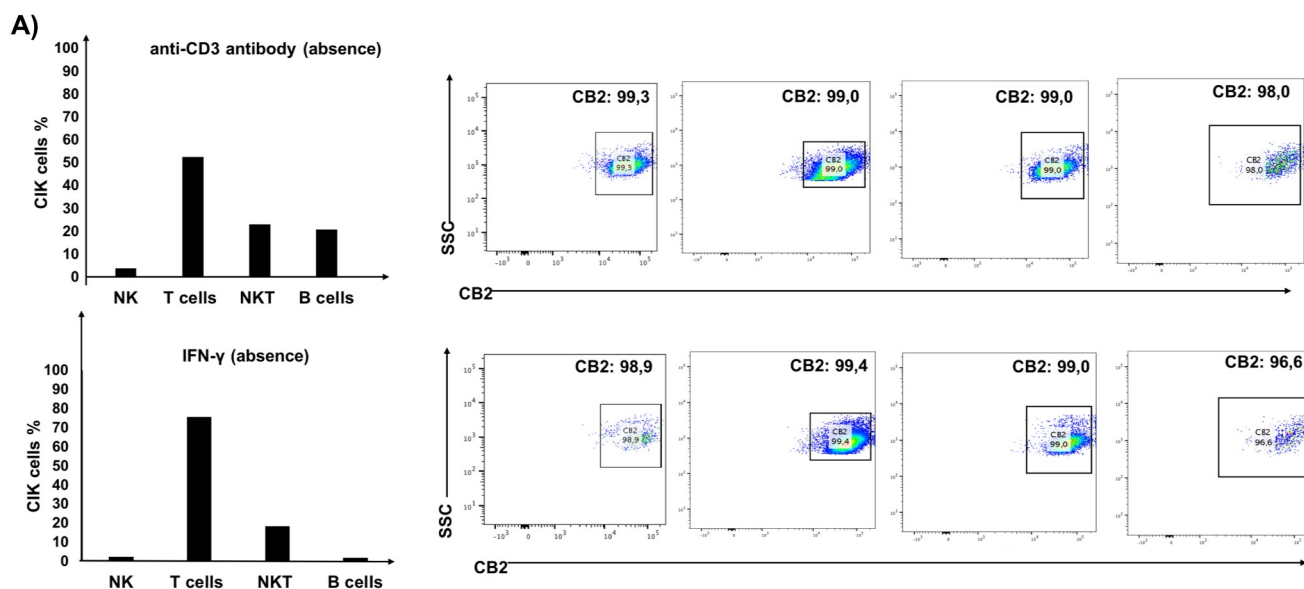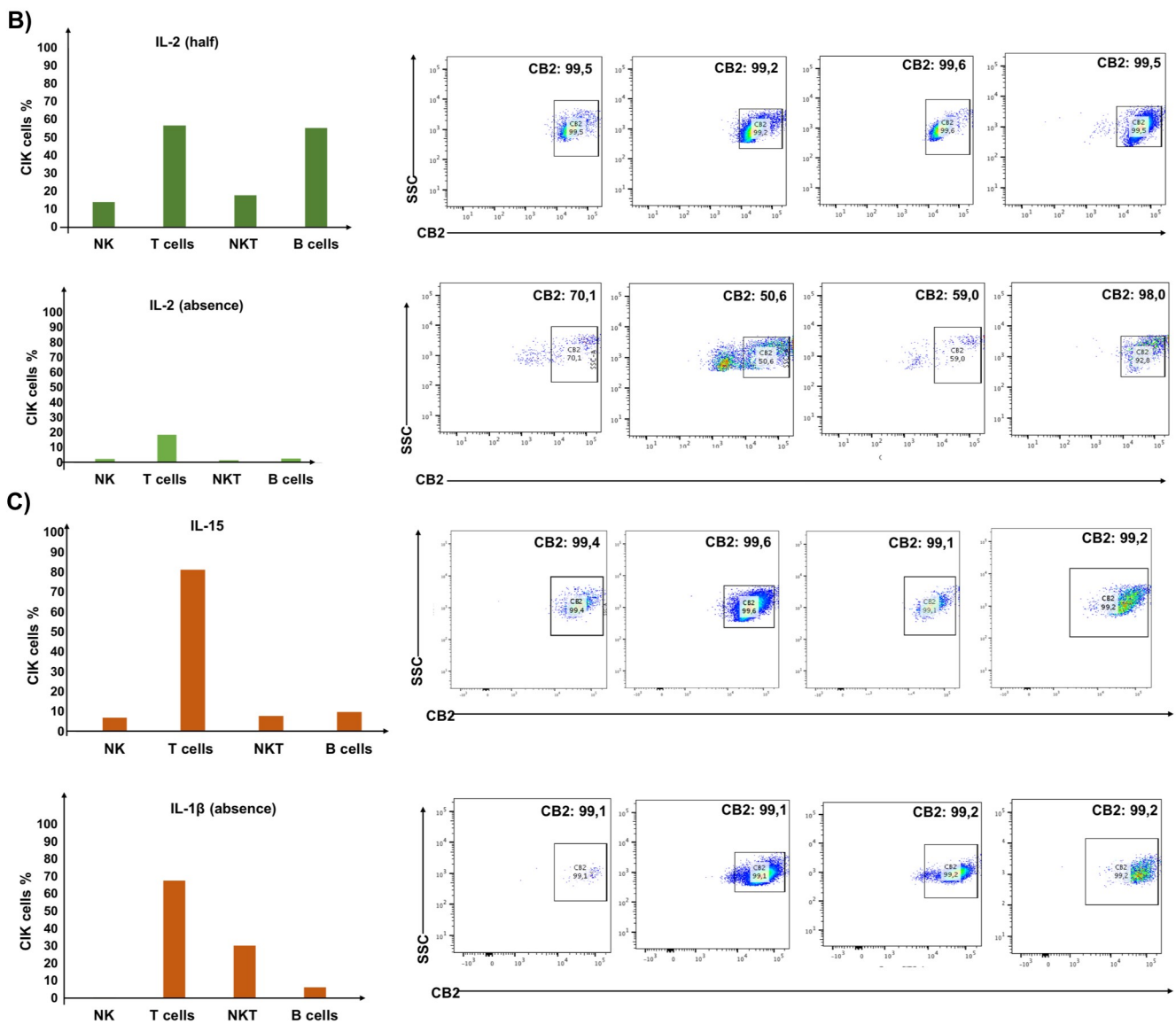

Figure 1. *Cont.*

Figure 1. Differential expression of CB2 receptor in the cell subsets of CIK cells. CIK cells were cultured (**A**) in the absence of anti–CD3 antibody (**upper** panel) and IFN–γ (**lower** panel), (**B**) in half of the amount of IL–2 (**upper** panel) and in the absence of IL–2 (**lower** panel), and (**C**) with IL–15 (**upper** panel) and in the absence of IL–1β (**lower** panel). In all experiments, CIK cells were immunophenotyped at day 14 by flow cytometry and the differential expression of CB2 receptor in the main cell subsets of human CIK cells, i.e., NKT, T, NK, and B cells were determined.

3.2. An Autophagosomal-Associated Scaffold Protein p62 Also Colocalizes with CB2 Receptors in CIK Cells and the PANC-1 Cell Line

As aforementioned, CB2 receptors colocalize with p62 vesicles mainly in the plasma membrane of transiently transfected HEK293 cells. Herein, we also investigated possible co-localizations of these two proteins in CIK cells and PANC-1 cells by using immunocyto-chemical studies and a 3D reconstruction modeling of confocal images. We observed that p62 vesicles were surrounded by CB2-positive areas (Figure 2). Particularly in CIK cells, reconstruction images showed that p62 vesicles were surrounded by CB2-positive areas at the surface membrane and also intracellularly (Figure 2A–D). In the case of PANC-1 cells, we used a segmentation algorithm and determined p62-positive regions that co-expressed CB2 (Figure 2E,F).
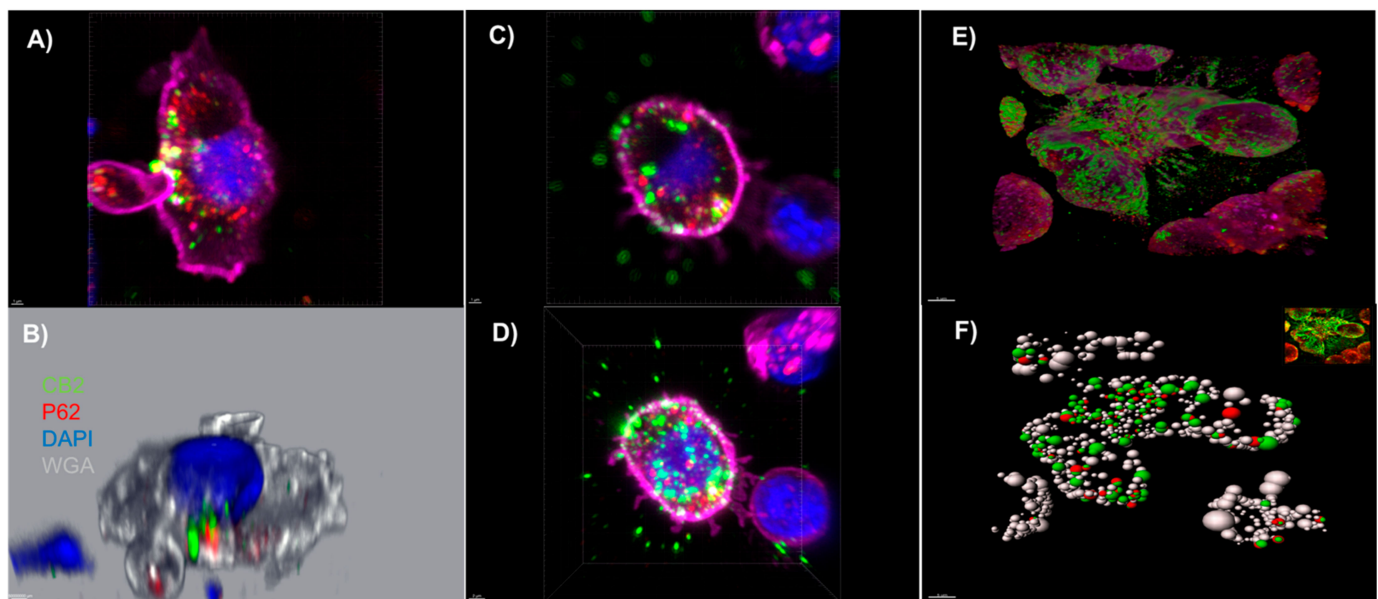
Figure 2. (**A**–**D**) Confocal light microscopy of CIK cells at day 14 expressing CB2 receptors. Immuno-histochemical staining of CB2 (green), p62 (red), and DAPI (blue). The membrane was stained by Texas-red conjugated wheat-germ-agglutinin (magenta) and DAPI revealed the localization of the nucleus. (**A**,**B**) Co-localization of CB2 receptors and p62 vesicles at the cell membrane which are in yellow due to the overlap of green and red. 3D reconstruction of confocal images to distinguish the CB2 receptor (green) out of the membrane (grey), and p62 vesicles (red) inside the membrane in close proximity to CB2 receptors; (**C**,**D**) co-localization of CB2 receptors and p62 vesicles intracellularly. The CB2 receptors have a different distribution in the cell membrane; (**E**,**F**) confocal light microscopy of PANC-1 pancreatic cancer cell line expressing CB2 receptors. Immunohistochemical staining of CB2 (green), p62 (red). The membrane was stained by Texas-red conjugated wheat-germ-agglutinin (magenta). 3D reconstruction modeling of confocal images using a segmentation algorithm to distinguish a single signal from different channels showing co-localization of CB2 receptors and p62 vesicles.

3.3. CIK Cells Showed a Low Level of Intracellular p-p38 and Donor Specific Variability in p-CREB

To determine potential effects of downstream mediators of CB2, such as phosphorylation of p38 and CREB, which presumably could indirectly affect the pleiotropic cytokines (IL-6/IL-10) that overlap with the CIK cell function. We next examined intracellular p-p38 expression in CIK cells immunophenotyped on days 7 and 14 of ex vivo expansion by flow cytometry (Figure 3). Interestingly, p-p38 was detectable only at low levels in the subset of T lymphocytes at day 7, whereas it was undetectable in other subsets at either day 7 or day 14 (Figure 3A,B). Similarly, we immunophenotyped PANC-1 cells and observed p-38 undetectable (Figure 3C). In the case of the second mediator (p-CREB), we incubated CIK cells (day 14) with cannabidiol at different concentrations of 1–20 µM and found a weak signal (Figure 3D). Notably, in the case of p-CREB, donor-specific variability was observed, with two donors showing a decrease in CREB phosphorylation at 1–3 µM and one at 1 µM compared to the untreated and DMSO control.
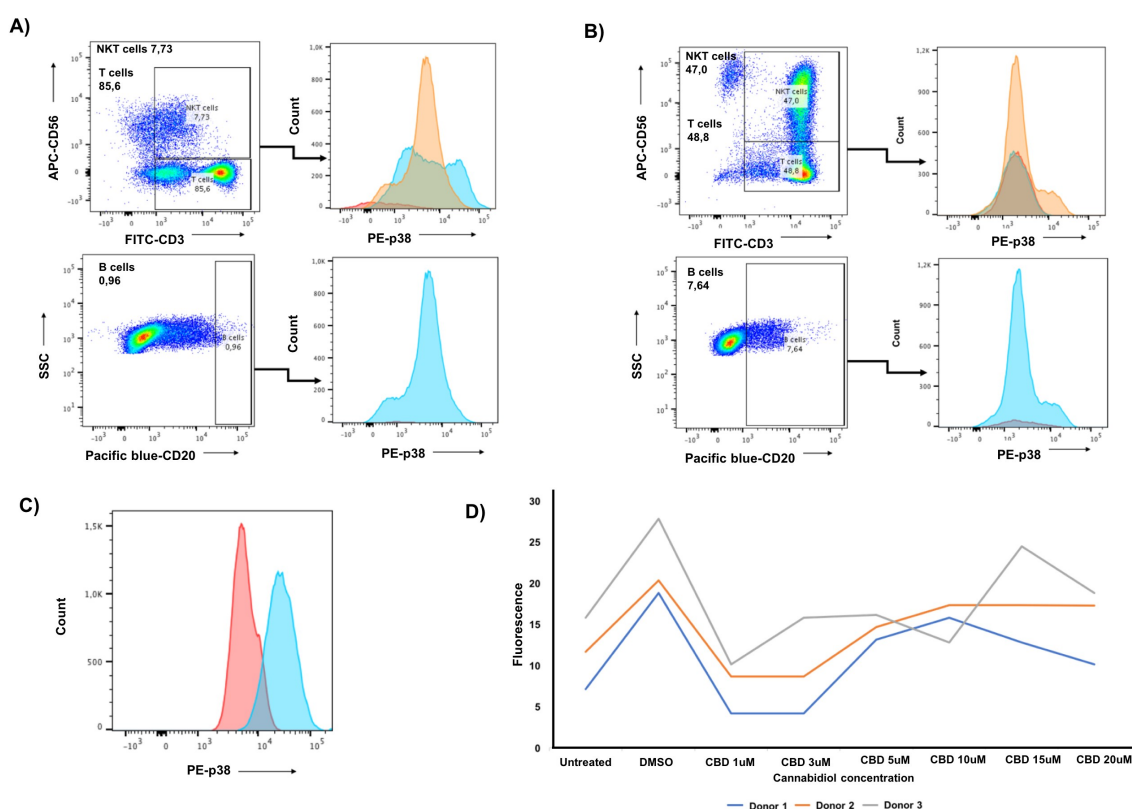
Figure 3. (**A**) The expression of p-p38 in the main cell subsets of human Cytokine-induced killer (CIK) cells, i.e., CD3⁺CD56⁺(NKT), CD3⁺CD56⁻ (T cells), and CD20⁺ B cells. Intracellular p–p38 expression was evaluated and the CIK cells were immunophenotyped at day 7 by flow cytometry. For the subsets CD3⁺CD56⁺(NKT) 7.73%, CD3⁺CD56⁻ (T cells) 85.6%, p–p38 expression (histogram representation) was 0% (red) and 3.0% (blue), respectively. The isotype is orange. For CD20⁺ B cells 0.96%, p–p38 expression was 0% (red). The isotype is blue. (**B**) Intracellular p–p38 expression was evaluated and the CIK cells were immunophenotyped at day 14 by flow cytometry. For the subsets CD3⁺CD56⁺(NKT) 47.0%, CD3⁺CD56⁻ (T cells) 48.8%, p–p38 expression (histogram representation) was % 0 (red) and 0% (blue), respectively. The isotype is orange. For CD20⁺ B cells 7,64%, p–p38 expression was 0% (red). The isotype is blue. (**C**) The expression of p–p38 in PANC-1 cell line. Intracellular p–p38 expression was evaluated, and the cells were immunophenotyped by flow cytometry. Histogram dotplot with PANC–1 cells (red) and isotype (blue). P–p38 was not detectable in PANC–1 cell line via flow cytometry. (**D**) Phosphorylation of CREB in CIK cells stimulated with cannabidiol from 1 μM to 20 μM for 30 min at 37 °C. The graph shows the mean of three independent experiments performed in technical triplicate, each with cells from a separate subject (three subjects in total). The data were normalized.

3.4. Cannabidiol Significantly Decreases the Viability of PANC-1 Cells and Significantly Increases the Cytotoxicity of CIK Cells against PANC-1 at Low Concentrations

Next, we measured the cell viability of PANC-1 cells exposed to various concentrations of CBD (1–20 μM) for 24 h at 37 °C. We observed significant decrease in the cell viability compared to the DMSO control (Figure 4A). Of interest, when cytotoxicity of PANC-1 cells exposed to different concentrations of CBD was assessed, a significant decrease in LDH release was observed at low concentrations (1 μM and 3 μM) and an increase was observed at high concentrations (15 μM) compared to the DMSO control (Figure 4B). Notably, no significant difference was observed when effector cells were cultured with target cells (PANC-1) E:T ratio of 10:1 and exposed to different CBD concentrations (1–20 μM) (Figure 4C). The LDH cytotoxicity experiment also showed no significant differences compared to the DMSO control (Figure 4D).
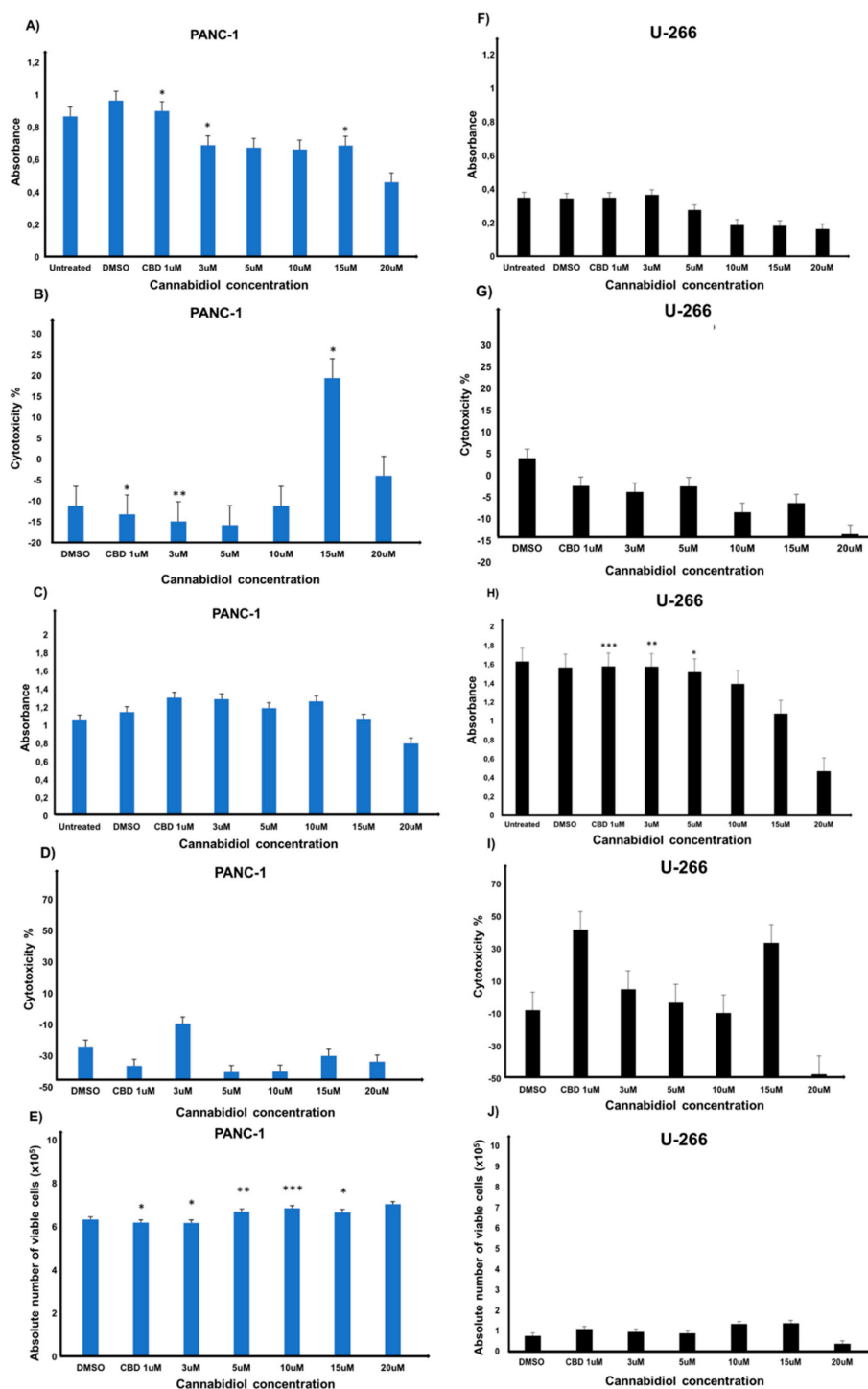
Figure 4. The cell viability in PANC–1 cells exposed to various concentrations of CBD by (**A**) CCK–8 assay and (**B**) LDH assay. The cell viability of the co–cultured CIKs and PANC–1 cells at E:T ratio of 10:1 by (**C**) CCK–8 assay and (**D**) LDH assay. (**E**) The absolute number of viable PANC–1 cells for each sample condition with cocultured CIKs and PANC–1 cells at an E:T ratio of 10:1. The cell viability in U–266 cells exposed to various concentrations of CBD by (**F**) CCK–8 assay and (**G**) LDH assay. The cell viability of the co–cultured CIKs and U–266 cells at E:T ratio of 10:1 by (**H**) CCK–8 assay and (**I**) LDH assay. (**J**) The absolute number of viable U–266 cells for each sample condition with cocultured CIKs and PANC–1 cells at an E:T ratio of 10:1 (* $p < 0.05$, ** $p < 0.01$, *** $p < 0.001$).

However, when effector cells were cocultured with target cells (PANC-1) E:T ratio of 10:1 and exposed to different concentrations of CBD (1–20 μM) for 24 h at 37 °C, a concentration-dependent inhibitory response was observed using flow cytometry analysis (Figure 4E)—thus suggesting that CBD significantly decreases the viability of PANC-1 cells presumably by increasing the cytotoxicity of CIK cells.

To determine whether this low effective CBD dose, which appears to be sufficient to stimulate cytotoxic function of CIK cells, is limited to pancreatic cells or if it could be a general phenomenon in cancer, we additionally tested myeloma cells. Particularly, we measured the cell viability (Figure 4F) and cytotoxicity (Figure 4G) of U-266 cells exposed to various concentrations of CBD (1–20 μM) for 24 h at 37 °C. No significant difference was observed compared to the DMSO control in both experiments. However, a significant difference was observed when effector cells were cultured with target cells (U-266) E:T ratio of 10:1 and exposed to different CBD concentrations (1–20 μM) (Figure 4H). It is worth noting a significant increase at 1 μM and 3 μM and a significant decrease at 5 μM compared to the DMSO control was observed. However, it remains difficult to distinguish between tumor cells and CIK cells. Notably, no significant difference was observed in the LDH release (Figure 4I) when effector cells were cultured with target cells (U-266) E:T ratio of 10:1 and exposed to different CBD concentrations (1–20 μM) and using flow cytometry analysis (Figure 4J) compared to the DMSO control.

4. Discussion

It has been well understood that genetic-epigenetic, inter/intra-individual heterogeneity and various yet to be known factors contribute to the complexity of cancer [19–21]. Nevertheless, the relative contribution of several immunotherapeutic approaches has helped to partially tackle this adverse effect of disease in the clinics. Among these approaches, cytokine-induced killer (CIK) cell therapy has played a pivotal role and raised the bar regarding treatment response due to its safe and efficient methodology [22–24]. The uniqueness of CIK cells is their encouraging synergetic effect with cancer associated inhibitors/compounds in preclinical models since cannabinoids have been the subject of intensive cancer research, in particular cannabinoid receptor 2 (CB2) due to its expression in cells of the immune system where CIK cells also play an important role. To date, no study has thoroughly investigated the combinatorial impact of CBD and CIK cells, particularly in pancreatic cancer (PC). It is worth noting that the implication of cannabinoids in PC can be from different CB ligands from the study where the combination of synthetic cannabinoids and gemcitabine synergistically trigger the inhibition of PC cells growth by a ROS-mediated autophagy induction involving the AMP-activated protein kinase (AMPK) [25,26]. Considering this, herein, we sought to investigate whether inducing CIK cells with CBD can enhance their cytotoxicity in pancreatic cells. Besides our major focus on the PC cellular model (PANC-1 cell line), we also used myeloma cells (U-266 cell line) as a proof of concept.

In our analysis, we first found that IL-2 primarily determines the expression of CB2 receptor on CIK cells. This was clearly evident from the analyses when both surface and intracellular CB2 expression were confirmed on CIK cells generated from PBMCs of healthy volunteers and respective percentage of CD3$^+$CD56$^+$, CD3$^+$CD56$^-$, and CD3$^-$CD56$^+$ CIK cells was quite distinguishable in all groups. Importantly, the percentages of CB2 positive cells always remains high, regardless of co-culturing with any CIK cell mediators (anti-CD3 antibody, IFN-γ, IL-2, IL-15, and IL-1β). The cytokine cocktail includes IL-2 to promote survival and activation of cytolytic effector function of CIK cells, and IL-15, which is capable of further activating CIK cells and shares common signaling components with IL-2, e.g., activation of the Jak/STAT signaling pathways. Next, we investigated whether CB2 receptors colocalize with p62 vesicles in CIK cells and PANC-1 cells, as it has been previously reported in HEK293 cells [17]. Our analysis clearly showed that p62 vesicles were surrounded by CB2-positive areas at the surface membrane and also intracellularly in CIK cells, while p62-positive regions were co-expressed with CB2 in PANC-1 cells. Given that CIK cells are heterogenous, here it is unclear which subtype of CIK cells contributes

predominantly towards the localization with p62. Previously, it has been shown that CB2 induces the phosphorylation of p38 MAPKs, downstream CREB phosphorylation and induction of IL-6, IL-10 cytokine secretion in human primary leukocytes [18]. Therefore, we also examined intracellular p-p38 expression in CIK cells immunophenotyped on day 7 and day 14 of ex vivo expansion. Interestingly, we found that CIK cells showed a low level of intracellular p-p38, primarily in the subset of T lymphocytes at day 7, while, in the case of p-CREB, we found a weak and variable signal among donors when CIK cells (day 14) were incubated with CBD. This clearly indicated that CBDs (mainly at low concentration) are sufficient to stimulate the cytotoxic function of CIK cells without exerting the downstream mediators like p38 and/or CREB, particularly in the pancreatic adenocarcinoma cell line. Nevertheless, whether the expression of other molecules such as perforin or granzyme B is also affected in this crosstalk between CIK, and CBD requires further validation. It is worth noting that cell viability and cytotoxicity of PANC-1 cells were also found to be significantly decreased when they were exposed to various concentrations of CBD (1–20 μM) for 24 h at 37 °C. Interestingly, when CIK cells were co-cultured, a concentration-dependent inhibitory response was observed in these cells—thus suggesting that CBD (in low concentration) presumably increased the cytotoxicity of CIK cells, which in turn negatively impacted the viability of PANC-1 cells. Despite this low effective CBD dose, impact is limited to pancreatic cells or it is a general phenomenon in cancer, we additionally tested myeloma cells. Of interest, like PC cells, a significant difference was observed when effector cells were cultured with target cells (U-266) E:T ratio of 10:1 and exposed to different CBD concentrations (1–20 μM)—hence confirming that a low dose of CBD impacted in a similar way in both PC and myeloma cells, presumably via CIK cells.

Here, it is also important to mention the limitation of the study like using multiple cell lines with a varied genetic background would provide more detailed insights. Certainly, an in vivo validation of CBD-CIK crosstalk in a preclinical model is warranted. Still, ours is the first study to show that a low dose of pure cannabidiol is sufficient to stimulate the cytotoxic function of CIK without exerting any associated mediator. As CIK cell therapy is safe, introducing pure cannabidiol particularly for the non-respondent patients may help to increase the therapeutic response.

5. Conclusions

A low dose of pure cannabidiol (CBD) is sufficient to stimulate the cytotoxic function of CIK cells in cancer cells, primarily in pancreatic and myeloma cells.

References

1. Sharma, A.; Liu, H.; Herwig-Carl, M.C.; Chand Dakal, T.; Schmidt-Wolf, I.G.H. Epigenetic Regulatory Enzymes: Mutation Prevalence and Coexistence in Cancers. *Cancer Investig.* **2021**, *39*, 257–273. [CrossRef] [PubMed]
2. Sharma, A.; Schmidt-Wolf, I.G.H. 30 years of CIK cell therapy: Recapitulating the key breakthroughs and future perspective. *J. Exp. Clin. Cancer Res.* **2021**, *40*, 388. [CrossRef] [PubMed]
3. Li, Y.; Sharma, A.; Bloemendal, M.; Schmidt-Wolf, R.; Kornek, M.; Schmidt-Wolf, I.G.H. PD-1 blockade enhances cytokine-induced killer cell-mediated cytotoxicity in B-cell non-Hodgkin lymphoma cell lines. *Oncol. Lett.* **2021**, *22*, 613. [CrossRef] [PubMed]
4. Stephan, D.; Weiher, H.; Schmidt-Wolf, I.G.H. CIK Cells and HDAC Inhibitors in Multiple Myeloma. *Int. J. Mol. Sci.* **2017**, *18*, 945. [CrossRef]
5. Seltzer, E.S.; Watters, A.K.; MacKenzie, D., Jr.; Granat, L.M.; Zhang, D. Cannabidiol (CBD) as a Promising Anti-Cancer Drug. *Cancers* **2020**, *12*, 3203. [CrossRef]
6. Kovalchuk, O.; Kovalchuk, I. Cannabinoids as anticancer therapeutic agents. *Cell Cycle* **2020**, *19*, 961–989. [CrossRef]
7. Garofano, F.; Schmidt-Wolf, I.G.H. High Expression of Cannabinoid Receptor 2 on Cytokine-Induced Killer Cells and Multiple Myeloma Cells. *Int. J. Mol. Sci.* **2020**, *21*, 3800. [CrossRef]
8. Zhang, Y.; Schmidt-Wolf, I.G.H. Ten-year update of the international registry on cytokine-induced killer cells in cancer immunotherapy. *J. Cell. Physiol.* **2020**, *235*, 9291–9303. [CrossRef]
9. Garofano, F.; Gonzalez-Carmona, M.A.; Skowasch, D.; Schmidt-Wolf, R.; Abramian, A.; Hauser, S.; Strassburg, C.P.; Schmidt-Wolf, I.G.H. Clinical Trials with Combination of Cytokine-Induced Killer Cells and Dendritic Cells for Cancer Therapy. *Int. J. Mol. Sci.* **2019**, *20*, 4307. [CrossRef]
10. Pagano, C.; Navarra, G.; Coppola, L.; Bifulco, M.; Laezza, C. Molecular Mechanism of Cannabinoids in Cancer Progression. *Int. J. Mol. Sci.* **2021**, *22*, 3680. [CrossRef]
11. Nüsgen, N.; Goering, W.; Dauksa, A.; Biswas, A.; Jamil, M.A.; Dimitriou, I.; Sharma, A.; Singer, H.; Fimmers, R.; Fröhlich, H.; et al. Inter-locus as well as intra-locus heterogeneity in LINE-1 promoter methylation in common human cancers suggests selective demethylation pressure at specific CpGs. *Clin. Epigenetics* **2015**, *7*, 17. [CrossRef] [PubMed]
12. Schlick, K.; Kiem, D.; Greil, R. Recent Advances in Pancreatic Cancer: Novel Prognostic Biomarkers and Targeted Therapy-A Review of the Literature. *Biomolecules* **2021**, *11*, 1469. [CrossRef] [PubMed]
13. Xu, Z.; Hu, K.; Bailey, P.; Springfeld, C.; Roth, S.; Kurilov, R.; Brors, B.; Gress, T.; Buchholz, M.; An, J.; et al. Clinical Impact of Molecular Subtyping of Pancreatic Cancer. *Front. Cell Dev. Biol.* **2021**, *9*, 743908. [CrossRef] [PubMed]
14. Rawla, P.; Sunkara, T.; Gaduputi, V. Epidemiology of Pancreatic Cancer: Global Trends, Etiology and Risk Factors. *World J. Oncol.* **2019**, *10*, 10–27. [CrossRef]
15. Fogli, S.; Nieri, P.; Chicca, A.; Adinolfi, B.; Mariotti, V.; Iacopetti, P.; Breschi, M.C.; Pellegrini, S. Cannabinoid derivatives induce cell death in pancreatic MIA PaCa-2 cells via a receptor-independent mechanism. *FEBS Lett.* **2006**, *580*, 1733–1739. [CrossRef]
16. Carracedo, A.; Gironella, M.; Lorente, M.; Garcia, S.; Guzmán, M.; Velasco, G.; Iovanna, J.L. Cannabinoids induce apoptosis of pancreatic tumor cells via endoplasmic reticulum stress-related genes. *Cancer Res.* **2006**, *66*, 6748–6755. [CrossRef]
17. Sharaf, A.; Mensching, L.; Keller, C.; Rading, S.; Scheffold, M.; Palkowitsch, L.; Djogo, N.; Rezgaoui, M.; Kestler, H.A.; Moepps, B.; et al. Systematic Affinity Purification Coupled to Mass Spectrometry Identified p62 as Part of the Cannabinoid Receptor CB2 Interactome. *Front. Mol. Neurosci.* **2019**, *12*, 224. [CrossRef]
18. Saroz, Y.; Kho, D.T.; Glass, M.; Graham, E.S.; Grimsey, N.L. Cannabinoid Receptor 2 (CB(2)) Signals via G-alpha-s and Induces IL-6 and IL-10 Cytokine Secretion in Human Primary Leukocytes. *ACS Pharmacol. Transl. Sci.* **2019**, *2*, 414–428. [CrossRef]
19. Liu, H.; Li, H.; Luo, K.; Sharma, A.; Sun, X. Prognostic gene expression signature revealed the involvement of mutational pathways in cancer genome. *J. Cancer* **2020**, *11*, 4510–4520. [CrossRef]
20. Sharma, A.; Reutter, H.; Ellinger, J. DNA Methylation and Bladder Cancer: Where Genotype does not Predict Phenotype. *Curr. Genom.* **2020**, *21*, 34–36. [CrossRef]
21. Sharma, A.; Biswas, A.; Liu, H.; Sen, S.; Paruchuri, A.; Katsonis, P.; Lichtarge, O.; Chand Dakal, T.; Maulik, U.; Gromiha, M.M.; et al. Mutational Landscape of the BAP1 Locus Reveals an Intrinsic Control to Regulate the miRNA Network and the Binding of Protein Complexes in Uveal Melanoma. *Cancers* **2019**, *11*, 1600. [CrossRef] [PubMed]
22. Shirjang, S.; Alizadeh, N.; Mansoori, B.; Mahmoodpoor, A.; Kafil, H.S.; Hojjat-Farsangi, M.; Yousefi, M. Promising immunotherapy: Highlighting cytokine-induced killer cells. *J. Cell. Biochem.* **2019**, *120*, 8863–8883. [CrossRef] [PubMed]
23. Zhang, Y.; Ellinger, J.; Ritter, M.; Schmidt-Wolf, I.G.H. Clinical Studies Applying Cytokine-Induced Killer Cells for the Treatment of Renal Cell Carcinoma. *Cancers* **2020**, *12*, 2471. [CrossRef]
24. Zhang, Y.; Sharma, A.; Weiher, H.; Schmid, M.; Kristiansen, G.; Schmidt-Wolf, I.G.H. Clinical Studies on Cytokine-Induced Killer Cells: Lessons from Lymphoma Trials. *Cancers* **2021**, *13*, 6007. [CrossRef] [PubMed]
25. Dando, I.; Donadelli, M.; Costanzo, C.; Dalla Pozza, E.; D'Alessandro, A.; Zolla, L.; Palmieri, M. Cannabinoids inhibit energetic metabolism and induce AMPK-dependent autophagy in pancreatic cancer cells. *Cell Death Dis.* **2013**, *4*, e664. [CrossRef]
26. Donadelli, M.; Dando, I.; Zaniboni, T.; Costanzo, C.; Dalla Pozza, E.; Scupoli, M.T.; Scarpa, A.; Zappavigna, S.; Marra, M.; Abbruzzese, A.; et al. Gemcitabine/cannabinoid combination triggers autophagy in pancreatic cancer cells through a ROS-mediated mechanism. *Cell Death Dis.* **2011**, *2*, e152. [CrossRef] [PubMed]

3.3 Publication 3: Presence of the Transmembrane Protein Neuropilin in Cytokine-Induced Killer Cells

42

Presence of the Transmembrane Protein Neuropilin in Cytokine-induced Killer Cells

EUGENIA V. DÍEZ GARCÍA DE OLALLA[1,2], FRANCESCA GAROFANO[1], HANS WEIHER[2],
MICHAEL MUDERS[3], SARAH FÖRSTER[3] and INGO G.H. SCHMIDT-WOLF[1]

[1]Department of Integrated Oncology, CIO Bonn, University of Bonn, Bonn, Germany;
[2]Department of Immunology and Cell Biology, Bonn-Rhein-Sieg
University of Applied Sciences, Rheinbach, Germany;
[3]Rudolf-Becker-Laboratory, Institute of Pathology, University of Bonn, Bonn, Germany

Abstract. *Background/Aim: Cytokine-induced killer (CIK) cells are a heterogenous population of immune cells showing promising applications in immunotherapeutic cancer treatment. Neuropilin (NRP) proteins have been proven to play an important role in cancer development and prognosis. In this study, CIK cells were tested for expression of NRPs, transmembrane proteins playing a role in the proliferation and survival of cancer cells. Materials and Methods: CIK cells were analyzed at different time points via flow cytometry and quantitative real-time polymerase chain reaction for neuropilin expression. Results: Phenotyping results showed CIK cells having developed properly, and low levels of NRP2 were detected. On the other hand, no NRP1 expression was found. Two cancer cell lines were tested by flow cytometry: A549 cells expressed NRP1 and NRP2; U251-MG cells expressed high amounts of NRP2. CIK cell showed low levels of NRP2 expression on day 14. Conclusion: The presence of NRP2, but not NRP1, was shown for CIK cells. Recognizing NRP2 in CIK cells might help to improve CIK cell cytotoxicity.*

Neuropilins (NRPs) are non-tyrosine kinase glycoproteins expressed on the surface of cells of all vertebrate animals. There are two main molecules, NRP1 and NRP2 (located on different genes), which act as co-receptors for certain molecules. NRPs bind vascular endothelial growth factors (VEGFs), class III semaphorins, transforming growth factor beta, other growth factors and many more molecules (1).

Correspondence to: Ingo G.H. Schmidt-Wolf, Department of Integrated Oncology, University Hospital Bonn, Venusberg-Campus 1, 53127 Bonn, Germany. Tel: +49 22828717050; Fax: +49 2282879080059, e-mail: ingo.schmidt-wolf@ukbonn.de

Depending on what they bind, different pathways/signals are either induced or up-regulated. Regarding their effects on tumor cells, interactions of class III semaphorins and NRPs/plexins on cancer cells have been reported to induce inhibition of proliferation, migration, angiogenesis and immune responses (2). On the other hand, when VEGF molecules interact with NRPs, cell survival, proliferation, migration, angiogenesis and metastasis are induced (1).

Previous studies have focused on the role of NRPs on cancer cells, finding a pattern that highlights a positive correlation between the expression of NRPs in tumor cells and the malignancy of the same (1-3). Lal Goel *et al.* found that NRP-2 is associated with high-grade prostate cancer (4), it was also found to be a prognostic marker for survival in prostate cancer (5). Another study showed how the silencing of NRP1 in non-small cell lung carcinomas reduced proliferation and increased radiosensitivity of the tumor cells both *in vitro and in vivo* (6). Therefore, NRPs are becoming a protein of increasing importance in regard to oncology research.

Cytokine-induced killer cells (CIK) are expanded *ex-vivo* from peripheral blood mononuclear cells (PBMCs) of a patient's blood. They were firstly characterized by Schmidt-Wolf *et al.* in 1991 (7) and have been the focus of various prospective oncology therapies since (8). They have certain characteristic features which make them great candidates for adoptive immunotherapy: They are able to lyse tumor cells independently of the major histocompatibility complex, their proliferation rate is also higher than conventional lymphokine-activated killer cells (9), and they are readily available, quick and easy to generate, as well as being relatively cheap.

CIK cells are a heterogenous population composed of natural killer (NK) cells, T-cells and NK T-cells. The phenotype of CIK cells is determined based on the surface markers they express. NK cells express neural cell adhesion molecule (NCAM1 or CD56) but not CD3, T-cells express CD3 but not NCAM1, and NK T-cells, the most cytotoxic sub-group, express both of these molecules. Once isolated

CIK cells are mature, they can be analyzed to determine their phenotype (10). When characterizing CIK cells, two T-cell markers are also looked for: CD4 and CD8. CD4 is a marker of helper T-cells, which recruit cytotoxic cells which are CD8^{+} (11). Therefore, CD4^{+} and CD8^{+} populations of CIK cells are expected.

These cells are generated by isolation of PBMCs from a patient's blood and by cytokine addition, as described in the literature (7, 12). Briefly, PBMCs are isolated, monocytes and granulocytes are eliminated and finally CIK expansion is induced by the addition of interleukin-2 (IL2), IL1β, anti-CD3 and interferon-γ.

Since NRPs have been proven to play a role in up-regulating signals involved with key pathways in cancer cells, it was considered to be of interest to determine whether NRPs are present in CIK cells. Therefore, the aim of this study was to experimentally determine the presence or absence of NRP1 and NRP2 in CIK cells through flow cytometric analysis and quantitative real-time polymerase chain reaction (RT-qPCR).

Materials and Methods

Cell lines, cell cultures and reagents. CIK cells were generated from buffy coats of healthy donors as explained in the literature (7) using the following reagents: Phosphate buffered saline (PBS) (PAN Biotech, Aidenbach, Germany), ethylenediamine tetra-acetic acid (ITW Reagents, Darmstadt, Germany), pancoll (PAN Biotech), distilled water (Gibco/Thermo Fisher Scientific, Waltham, MA, USA), erythrocyte lysis buffer (BioLegend, San Diego, CA, USA), recombinant human interleukin-2 (ImmunoTools, Friesoythe, Germany), recombinant human interferon gamma (ImmunoTools), recombinant human interleukin-1-beta (ImmunoTools) and mouse anti-human CD3 monoclonal antibody (eBioscience - Thermo Fisher Scientific). The buffy coat was stored for a maximum of 24 hours at 4°C until CIK cell isolation. The CIK cells were incubated at 37°C, with 5% CO_2 and 95% humidity and kept in a T-175 flask at a density of 1-2×10^6 cells/ml with RPMI 1640 (PAN Biotech) medium supplemented with 10% fetal bovine serum (FBS) (Sigma-Aldrich, Oakville, ON, Canada) and 1% penicillin/streptomycin (Gibco/Thermo Fisher Scientific) as well as 1 M HEPES (PAN Biotech). The medium was changed every 3-4 days and from day 14, the cells were considered mature CIK cells. The tumor cell line A549 (DSMZ, Braunschweig, Germany), a lung cancer cell line, was cultured in a T-75 flask with 10 ml of RPMI 1640 medium supplemented with 10% FBS and 1% penicillin/streptomycin. The media was changed every 3-4 days and when the cells reached an observable confluence of around 90%, the cell line was seeded at a density of 0.1-0.5×10^6 cells/ml. The cells were incubated at 37°C, with 5% CO_2 and 95% humidity. The glioblastoma cell line U251-MG (Sigma-Aldrich) was acquired as a cell pellet ready to be thawed and used for flow cytometry antibody-staining. These cells were routinely checked for mycoplasma infection.

Flow cytometry and phenotyping of CIK cells. The cells were prepared for phenotyping at day 0, 1 and 14 onward, by creating a single-cell suspension in PBS at a density of 2×10^7 cells/ml. A staining buffer was also prepared: 0.1 g of bovine serum albumin (Sigma-Aldrich) in 10 ml of PBS. In each tube, 50 μl of the staining buffer were added, as well as 50 μl of the cell suspension. Additionally, making sure to work under dim lighting, monoclonal antibodies were added at the recommended concentrations: for fluorescein isothiocyanate (FITC)-conjugated mouse anti-human CD3, phycoerythrin-conjugated mouse anti-human neural cell adhesion molecule (NCAM1), allophycocyanin-conjugated mouse anti-human CD4 and Brilliant Violet 421™ mouse anti-human CD8a, 1 μl was added per tube (all BioLegend); for Pacific Blue™-conjugated mouse anti-human CD20 (BioLegend), FITC-conjugated mouse anti-human NRP1 (CD304) (BioLegend) and AF488-conjugated mouse anti-human NRP2 (R&D systems, Minneapolis, MN, USA), 5 μl were added per tube. Moreover, the tubes were kept on ice in the dark for 20 min. Afterwards, the cells were washed twice with 2 ml of PBS by centrifuging at 405×*g* for 5 min. The pellet was resuspended in 500 μl of PBS. The samples were then analyzed with BD FACS CANTO II and FACS DIVA program (BD Biosciences, San Jose, CA, USA) as explained in the literature (13). The software used to analyze and process the data was FlowJo 10.4.0 (FlowJo-BD Biosciences).

RNA isolation and cDNA synthesis. For RNA isolation, CIK cells from the same batch were used on day 0 and day 14, RNeasy mini kit and RNA-free DNase I kit (both from Qiagen, Venlo, the Netherlands) were used and the company's protocol was followed. In regard to the cDNA synthesis, the protocol from the manufacturer (Thermo Fisher Scientific) of the following reagents was followed: 5X reaction buffer, RiboLock RNase inhibitor (200 U/μl), random hexamer primer, dNTP mix, ReverseAid H Minus Reverse Transcriptase (200 U/μl) and nuclease-free water (Qiagen). A thermocycler (AnalytikJena, Jena, Germany) was used for incubation at 25°C for 10 min, then at 42°C for 60 min and lastly at 70°C for 10 min. The cDNA was stored at −20°C until further use.

Quantitative reverse transcriptase–polymerase chain reaction (RT-qPCR). Following the manufacturer's protocol from Thermo Fisher Scientific for RT-qPCR with SYBR green, the following reagents and instruments were used: a water-bath (Memmert, Schwabach, Germany), vortex machine (Velp Scientifica, Usmate Italy) nuclease-free water, maxima SYBR green (Thermo Fisher Scientific), forward primer, and reverse primer, a 96-well plate, a centrifuge (AG Schorle, BMZ, Universitätsklinikum Bonn, Germany), and an RT-qPCR instrument (4351106, Applied Biosystems -Thermo Fisher Scientific). Three genes were tested: *NCAM1*, *NRP2* and peptidylprolyl isomerase A (*PPIA*; as a positive control). The primers used were the following: *NRP2*: forward: 5'ACCAGAACTGCG AGTGGATT3', reverse: 5'CGATGTTCCCACAGTGTTTG3'; *NCAM1*: forward: 5'GACCAGGTGGAGCCATACTC3', reverse: 5'TTACGGCGTACG TTGTTTCG3'; *PPIA*: forward: 5'GCTGGACCCAACACAAA TGG3', reverse: 5'GGCCTCCACAAT ATTCATGCCT3'. Triplicates were prepared for each sample, two cell types were tested (CIK and U251-MG) and the CIK cells were tested at two time points: day 0 and day 14. A negative control, with nuclease-free water instead of cells, was also used, resulting in a total of 36 samples. The RT-qPCR was run as follows: one cycle of 50°C for 2 min; one cycle of 95°C for 10 min; 40 cycles of 95°C for 10 min, 63°C for 15 s and 60°C for 1 min; one cycle of 95°C for 15 s, 60°C for 1 min and 95°C for 30 s; one cycle of 60°C for 15 s. After the run and after obtaining the results, the expression of the genes in CIK cells relative to those in U251-MG cells, as well as relative to day 0 CIK cells, was calculated
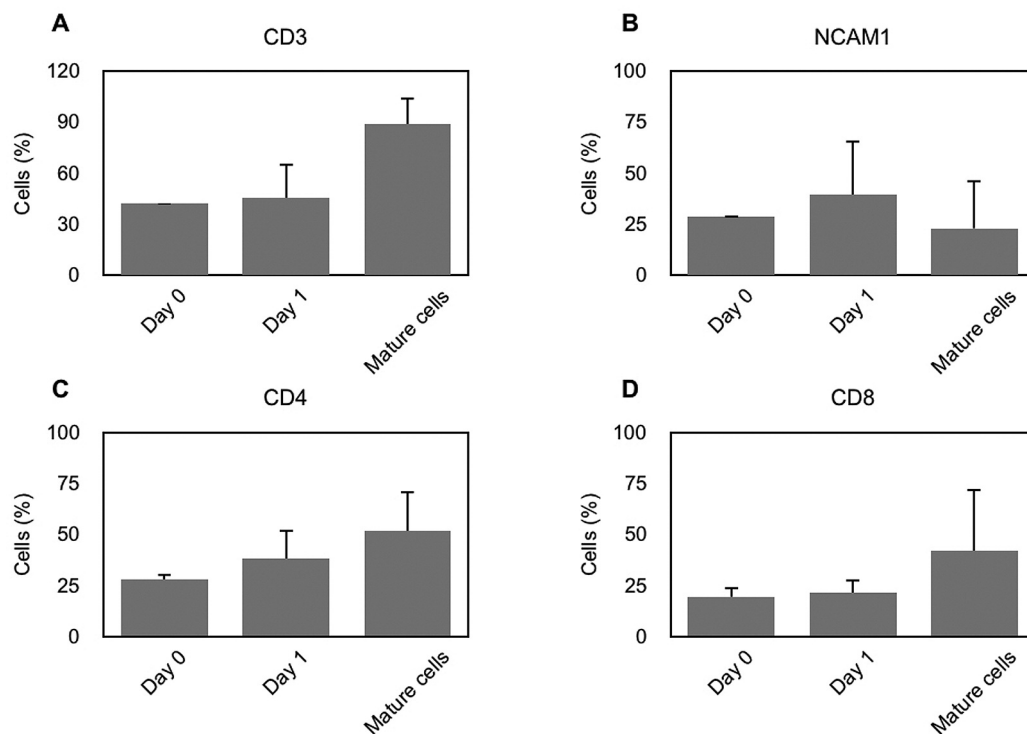
Figure 1. *Phenotyping of cytokine-induced killer (CIK) cells (single markers) by flow cytometry. The percentage of CIK cells expressing CD3 (A), neural cell adhesion molecule (NCAM1) (B), CD4 (C) and CD8 (D) at different time points of cell development. Data are presented as the mean±SD. The sample size on day 0 was two, day 1 three and for mature cells four.*

using the Ct values obtained and the formulae: $\Delta Ct = Ct_{target\ gene} - Ct_{housekeeping\ gene}$, $\Delta\Delta Cq = \Delta Ct_{treated} - \Delta Ct_{control}$, ratio $= 2^{(-\Delta\Delta Cq)}$; he SD was also calculated as shown in the protocol (14).

Statistical analysis. Descriptive data and graphics were prepared using Numbers (Apple, Cupertino, CA, USA). Sample means were calculated and reported with the standard deviation. Results are also presented as fold expression of the control, where one-fold represents the same level of expression as the control.

Results

Phenotyping of CIK cells through flow cytometry. The generated CIK cell population was characterized based on the number of cells expressing specific cell surface markers: CD3, NCAM1, CD4 and CD8. In Figure 1A, it can be observed that the percentage of cells expressing CD3 increased from day 0 to day 14. Figure 1B shows that the percentage of NCAM1$^+$ cells increased from day 0 to day 1, after which it decreased by day 14. Regarding Figure 1C, CD4$^+$ cells increased from day 0 to day 14. Lastly in Figure 1D, the proportion of CD8$^+$ cells also increased from day 0 to day 14. Figure 2 shows that the percentage of cells in the lymphocyte population increased with time up to day 14, whereas the populations of monocytes

and granulocytes decreased as the CIK cell population matured. It can also be seen that the population of CD3$^+$NCAM1$^+$ cells decreased on day 1, after which it increased. Regarding the populations of CD3$^+$CD4$^+$ and CD3$^+$CD8$^+$ cells, both increased with time.

Determination of NRP expression by flow cytometry. The levels of NRP1 and NRP2 expression were measured by flow cytometry using labelled antibodies. Two cell lines were taken as positive controls, U251-MG for NRP2 and A549 for NRP1 and NRP2. Different CIK cell batches were isolated and tested at different time points. In Figure 3, the results obtained for the expression of NRP1 and NRP2 in CIK cells and A549 cells can be seen. The graph shows the mean expression of all of the tested batches normalized against the antibody controls of each measurement which had identical isotypes to the tested antibodies. A549 cells had a level of NRP2 expression similar to that of CIK cells on both day 1 and day 14. On the other hand, NRP1 expression in CIK cells at all time points averaged the same or lower than the isotype control.

NRP2 mRNA detection through RT-qPCR. One batch of CIK cells was analyzed on days 0 and 14 through RT-
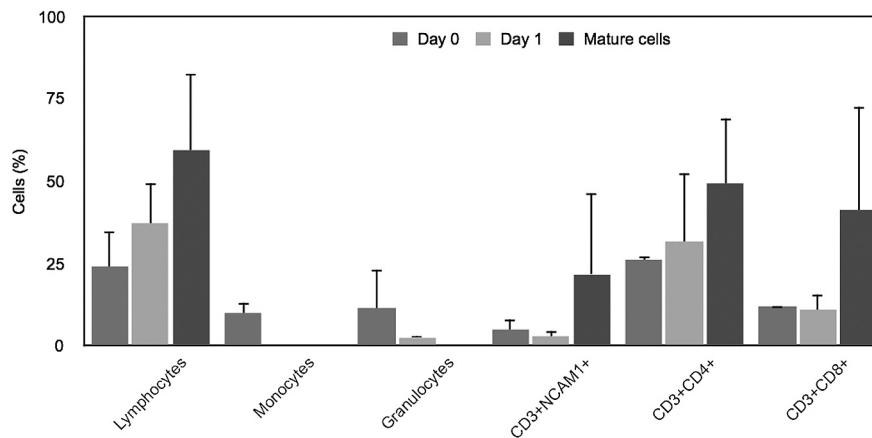
Figure 2. *Phenotyping of cytokine-induced killer (CIK) cells (double-positive markers) and peripheral blood mononuclear cell (PBMC) populations using CD3, CD4, CD8, and neural cell adhesion molecule (NCAM1) expression. CIK cells were analyzed on day 0, 1 and day 14 (mature cells). The different PBMC populations (lymphocytes, monocytes and granulocytes) were gated in the obtained fluorescence-activated cell sorting dot plot (FSC-A vs. SSC-A) and the percentage of cells belonging to those populations are than seen as a percentage. The percentage of double-positive populations, CD3+NCAM1+, CD3+CD4+ and CD3+CD8, are also shown. Data are presented as the mean±SD. The sample size on days 0 and 1 was three, and for mature cells was four.*
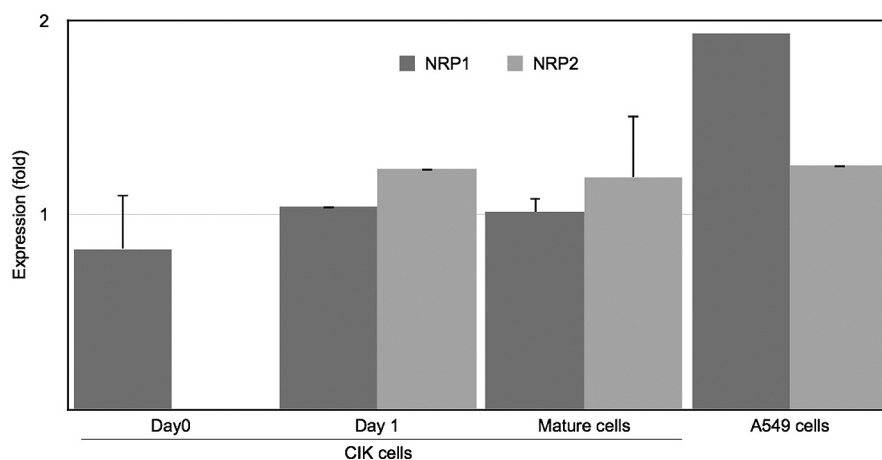

Figure 3. *Expression of neuropilin-1 (NRP1) and neuropilin-2 (NRP2) in A549 and cytokine-induced killer cells (CIK cells), normalized against the control antibody with identical isotype using flow cytometry. Fold expression is shown, where 1 equals the same level of expression as the control antibody with identical isotype. Data are presented as the mean±SD. The sample size for NRP1 in CIK cells on day 0 was two, on day 1 was one and for mature cells was two; for NRP2 no data were collected on day 0, on day 1 the sample size was one and for mature cells it was five. The sample size in A549 cells for NRP1 was two and for NRP2 was three.*

qPCR. As a positive control, the cell line U251-MG was also tested since it is a cell line that was shown to express a high amount of NRP2 (15). Three parameters were measured: Relative expression of *NRP2, NCAM1* and *PPIA*. The relative expression of the genes in CIK cells was compared to those of the positive control cell line U251-MG. The results can be seen in Table I. CIK cell expression was normalized firstly against the expression in U251-MG

cells. This showed the expression of *NRP2* increased from day 0 to day 14 but this was not very clear because the U251-MG cell line expressed both genes at a higher level. When expression was normalized against that of day 0 CIK cells, the pattern of expression was clearer. In Figure 4, the expression of NRP2 and NCAM1 in CIK cells on day 14 were normalized against the expression of those same genes on the same CIK cells at day 0. The results showed

Table I. *Quantitative real-time polymerase chain reaction results and calculated relative expression of neuropilin-1 (NRP1) and neural cell adhesion molecule (NCAM1) on cytokine-induced killer cells (CIK). ΔCt, ΔΔCt and ratio values were calculated as per the protocol (14) in the Materials and Methods section. The expression of the genes was normalized against U251-MG cells and against CIK cells on day 0. Peptidylprolyl isomerase A (PPIA) was used as a housekeeping gene. The sample size for all Ct values was three, except for CIK cells on day 0 and 14 testing NCAM1, where one outlier was excluded for each triplicate and therefore the sample sizes for each was two.*

Target	Sample		Mean Ct	Ct SD	ΔCt	ΔCt SD	ΔΔCt	ΔΔCt SD	Ratio	SD	ΔΔCt	ΔΔCt SD	Ratio	SD
NCAM1	U251-MG		21.690	0.190	3.820	0.236	0	0.236	1	0.1777	-	0.236	-	
	CIK cells	Day 0	27.415	0.120	3.805	0.134	–0.015	0.134	1.0105	0.0986	0	0.134	1	0.0976
		Day 14	24.875	0.601	3.535	0.651	–0.285	0.651	1.2184	0.6947	0.270	0.651	1.2058	0.6875
NRP2	U251-MG		19.490	0.060	1.620	0.152	0	0.152	1	0.1114	-	0.152	-	
	CIK cells	Day 0	36.930	0.000	13.320	0.060	11.700	0.060	0.0003	0.0000	0	0.060	1	0.0425
		Day 14	31.570	0.640	10.230	0.687	8.610	0.687	0.0026	0.0016	3.090	0.687	8.5150	5.1945
PPIA	U251-MG		17.870	0.140	-	-	-	-	-		-	-	-	
	CIK cells	Day 0	23.610	0.060	-	-	-	-	-		-	-	-	
		Day 14	21.340	0.250	-	-	-	-	-		-	-	-	

a clearer fold increase in expression of NRP2 from day 0 to day 14.

Discussion

NRPs have been proven to play a role in cancer progression and severity, and therefore it has become a protein of interest in oncology studies. In this report the focus was on the study of this transmembrane protein in a specific immune-system cell-type: CIK cells. These cells have been and are being studied with the purpose of using them for adoptive immune-therapies directed against cancer. Since as far as we are aware the presence of NRPs have never been reported on CIK cells, this study was focused on determining this. The two NRPs were tested: NRP1 and NRP2 and flow cytometry and RT-qPCR were performed. As a positive control, the cell lines A549 and U251-MG were used, since they have been already proven to express NRP1 and/or NRP2 (16, 17).

Firstly, the CIK cells to be tested were characterized by flow cytometry. The results can be seen in Figures 2 and 3. Of all CIK cells, 86.5% of the population are expected to express CD3, 28.5% NCAM1, 45.4% CD4 and 47.7% CD8 (10). The phenotyping results seen in Figure 1 of cell-surface marker expression are in accordance with the literature (10), despite our testing a relatively low number of cell batches. The error bars (representing the standard deviation of the mean) indicate for the broad range of the samples.

On day 0, a lower proportion of cells expressed CD3, NCAM1, CD4 and CD8 than did mature CIK cells, which is consistent with the literature (18). Regarding the results for day 1, the percentage of CD3+, CD4+ and CD8+ cells was higher in comparison to day 0, but lower than in mature CIK cells. The only discrepancy in Figure 1 can be seen for the percentage of CIK cells expressing NCAM1 on day 1, which
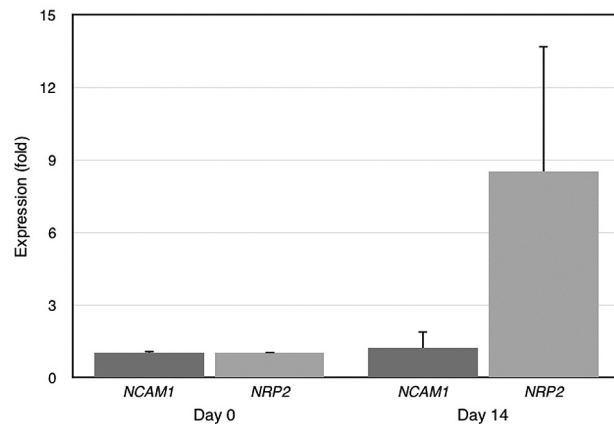

Figure 4. *Graph showing the relative expression of neuropilin-2 (NRP2) and neural cell adhesion molecule (NCAM1) on day 0 and day 14 in cytokine-induced killer cells (CIK). Expression in CIK and U251-MG cells was analyzed through quantitative real-time polymerase chain reaction using SYBR green as the reporting dye. The expression levels of CIK cells on day 14 were normalized against the expression of CIK cells on day 0. Data are presented as the mean±SD fold expression, where 1 represents the same expression as that at day 0.*

was higher on day 1 and day 0 than on day 14. Zhao *et al*. found similar results, where the percentage of NCAM1-expressing cells on day 0 was 26.8% but that in mature CIK cells was only 24% (18). This is a very small difference in percentage but similar results can also be seen in Figure 1 of this study, where on day 0, 28.9% of cells expressed NCAM1 while on day 14, 23% did. This leads to the conclusion that the natural expression pattern of NCAM1 in CIK cells is such that as cells mature, the NCAM1+ population decreases.

In this study, the population of lymphocytes increased as expected after day 0 (Figure 2), since the CIK cells are immune-system cells of the lymphocyte population. Monocytes were present on day 0, but not on days 1 and 14. This is due to monocytes being adherent cells, which by the protocol, are to be excluded on day 0 immediately before interferon-γ was added. Regarding granulocytes, the population disappeared after day 1 since the cytokine addition on that day makes the cells differentiate into lymphocytes. Figure 2, therefore, shows how the CIK cell batches used for the further experiments developed properly and according to literature (7).

Figure 2 also shows how the proportion of CD3⁺NCAM1⁺ cells decreased slightly from day 0 to day 1 and increased again on day 14. These findings are consistent with the literature (19), where the percentage of CD3⁺NCAM1⁺ cells was below 3% on day 0, decreased slightly on day 1 and then increased to around 35% on day 14. The results for CD3⁺CD4⁺ cells are slightly different from those of the literature (19), since on day 14, the population comprised around 50%, whereas in the literature the population decreased to about 20% on day 14. Lastly, the finding for the CD3⁺CD8⁺ population was similar to results in the literature for days 0 and 1 but on day 14, the obtained result was about 40%, whereas Meng *et al*. shows values of around 80%. This would mean that the cells used in this study were not as cytotoxic, since that characteristic is attributed to CD8⁺ cells (20). Still, there are publications in which the population of CD3⁺CD4⁺ cells was reportedly higher than that of CD3⁺CD8⁺ cells (21). Therefore, even though the CIK cells tested would not be as cytotoxic (20), they still fall within the parameters of previously reported CIK cells (21).

Another important point to consider when analyzing the results is that the phenotype of each CIK cell batch is patient-dependent (22) and, therefore, discrepancies in phenotyping between patients is expected. This can be seen when comparing the results in Figure 1B to the results in Figure 4. In Figure 1B, the average proportion of NCAM1⁺ cells can be seen to decrease from day 0 to day 14. However, the standard deviation was large on day 14, showing that the proportion of NCAM1⁺ cells in some batches increased as they matured. In Figure 4, on the other hand, an increase in NCAM1 expression from day 0 to day 14 can be seen.

The isolated CIK cells were tested by flow cytometry at different time points for the expression of the transmembrane NRP proteins. The cells lines U251-MG and A549 were also tested and taken as positive controls. The cell line U251-MG showed 36.6-fold expression of NRP2 when compared to the isotype. This is consistent with the literature (15). The A549 cell line also produced the expected results regarding NRP1 expression, concordant with the literature (6). However, NRP2 expression on A549 cells seemed to be very low, which is a discrepancy from the literature (23, 24), where NRP2 showed a clear positive band in western blots.

The expression level of NRP1 in CIK cells on day 0, 1 and 14 was equivalent to that of the isotype control. Regarding NRP2, on day 1 and day 14 expression was low. The standard deviation was large on day 14 for NRP2 since there was one sample in which expression was 1.76-fold. Since the phenotype of CIK cells varies from patient to patient, it could be hypothesized that NRP expression also does. From the results obtained, this cannot be proven since the sample size was too small, but it can be seen that NRP expression is not consistent in all CIK cell batches.

Further experiments would be necessary to determine whether the expression of NRPs in CIK cells is patient-dependent. In fact, Nasarre *et al*. obtained immunofluorescence results showing that not all A549 cells tested expressed similar amounts of NRP2 (24). It should therefore be considered that like A549 cells, NRP2 expression on CIK cells might vary from cell to cell. Another point to note is that flow cytometric analysis may not be the best method to determine the presence of NRP, since there might be intracellular presence of the protein. Therefore, future experiments should attempt to determine the presence of NRPs in CIK cells by other techniques such as western blotting. In fact, Nasarre *et al*. detected the presence of NRP2 in A549 cells through western blotting, and obtained clear positive results (24), as did Dong *et al*. (6), whereas through flow cytometry in our experiments, as seen in Figure 3, NRP2 seemed to be expressed at very low levels.

Lastly, one batch of CIK cells was taken to perform quantitative RT-qPCR, in which the samples were collected on day 0 and 14 after isolation. Since no cells were detected as being positive for NRP1, its RNA was not investigated. There was an 8.5-fold increase of NRP2 expression from day 0 to day 14 in CIK cells as seen in Figure 4 but the expression was still low when compared to that of the cell line U251-MG (Table I). Regarding the expression of NCAM1, the results in Table I and Figure 4 were as expected (10).

In future experiments, it would be of interest to retest the CIK cells using a cell line which expresses less NRP2, for example the A549 cell line. This cell line has already been tested through flow cytometry as seen in Figure 3, and would make a desirable future positive control. This cell line would also be a good choice since as seen in Figure 3, the A549 cells showed a level of NRP2 expression similar to that of CIK cells.

Finding proof of the presence of NRP2 on CIK cells might be advantageous for cancer therapy studies, since the presence of NRP has been proven to increase cancer progression and tumor cell migration, among others (1). Therefore, a possible way forward with this study might be to assess the importance of NRPs on CIK cells in regard to their cytotoxic effect on tumor cells. In other words, to see if there is a difference in the cytotoxicity of CIK cells against normal tumor cells *versus* against the same NRP-silenced cancer cells. Such a difference

could be advantageous for cancer therapy since, as previously described by Prud'homme *et al.* (1), the interaction of VEGF with NRPs on the membrane of cancer cells leads to cell survival, proliferation, migration, angiogenesis and metastasis of tumor cells. Therefore, it is possible that VEGF expressed by CIK cells (19) interacts with NRPs on tumor cells and may counteract the cytotoxic effect desired from immunogenic therapies. By silencing NRP, the susceptibility of the treated tumor cells to CIK cell therapy might be increased.

In conclusion, it can be stated that NRP2 is expressed on CIK cells. On the other hand, there is evidence to support the claim that NRP1 is not present on CIK cells. This might prove important in future studies to improve the cytotoxicity of CIK cells.

Conflicts of Interest

The Authors declare no conflicts of interest.

Authors' Contributions

EDGO prepared the cells, analyzed the samples, analyzed the data and wrote the article. FG aided in all practical work and guided the project as well as coordinated the experiments and corrected the article. HW corrected the article and aided in guiding the writing and editing. MM provided the U251-MG cell line as well as resources and guidance for the RT-qPCR experiment. SF aided in the preparation of samples for RT-qPCR and aided in analyzing the results. ISW provided resources, guided the project, supervised the development of the article, corrected and edited the article.

Acknowledgements

References

1 Prud'homme GJ and Glinka Y: Neuropilins are multifunctional coreceptors involved in tumor initiation, growth, metastasis and immunity. Oncotarget *3(9):* 921-939, 2012. PMID: 22948112. DOI: 10.18632/oncotarget.626

2 Grandclement C and Borg C: Neuropilins: A new target for cancer therapy. Cancers *3:* 1899-1928, 2011. PMID: 24212788. DOI: 10.3390/cancers3021899

3 Roy S, Bag AK, Singh RK, Talmadge JE, Batra SK and Datta K: Multifaceted role of neuropilins in the immune system: Potential targets for immunotherapy. Front Immunol *8:* 1228, 2017. PMID: 29067024. DOI: 10.3389/fimmu.2017.01228

4 Goel HL, Chang C, Pursell B, Leav I, Lyle S, Xi HS, Hsieh CC, Adisetiyo H, Roy-Burman P, Coleman IM, Nelson PS, Vessella RL, Davis RJ, Plymate SR and Mercurio AM: VEGF/neuropilin-2 regulation of BMI-1 and consequent repression of IGF-IR define a novel mechanism of aggressive prostate cancer. Cancer Discov *2:* 906-921, 2012. PMID: 22777769. DOI: 10.1158/2159-8290.CD-12-0085

5 Borkowetz A, Froehner M, Rauner M, Conrad S, Erdmann K, Mayr T, Datta K, Hofbauer LC, Baretton GB, Wirth M, Fuessel S, Toma M and Muders MH: Neuropilin-2 is an independent prognostic factor for shorter cancer-specific survival in patients with acinar adenocarcinoma of the prostate. Int J Cancer *146(9):* 2619-2627, 2019. PMID: 31509606. DOI: 10.1002/ijc.32679

6 Dong JC, Gao H, Zuo SY, Zhang HQ, Zhao G, Sun SL, Han HL, Jin LL, Shao LH, Wei W and Jin SZ: Neuropilin 1 expression correlates with the radio-resistance of human non-small-cell lung cancer cells. J Cell Mol Med *19:* 2286-2295, 2015. PMID: 26147006. DOI: 10.1111/jcmm.12623

7 Schmidt-Wolf IGH, Negrin RS, Kiem HP, Blume KG and Weissman IL: Use of a SCID mouse/human lymphoma model to evaluate cytokine-induced killer cells with potent antitumor cell activity. J Exp Med *174:* 139-149, 1991. PMID: 1711560. DOI: 10.1084/jem.174.1.139

8 Chen D, Sha H, Hu T, Dong S, Zhang J, Liu S, Cao H, Ma R, Wu Y, Jing C, Wang Z, Wu J and Feng J: Cytokine-induced killer cells as a feasible adoptive immunotherapy for the treatment of lung cancer. Cell Death Dis *9:* 366, 2018. PMID: 29511158. DOI: 10.1038/s41419-018-0404-5

9 Stephan D, Weiher H and Schmidt-Wolf IGH: CIK cells and HDAC inhibitors in multiple myeloma. Int J Mol Sci *18:* 945, 2017. PMID: 28468247. DOI: 10.3390/ijms18050945

10 Schmidt-Wolf IGH, Lefterova P, Mehta BA, Fernandez LP, Huhn D, Blume KG, Weissman IL and Negrin RS: Phenotypic characterization and identification of effector cells involved in tumor cell recognition of cytokine-induced killer cells. Exp Hematol *21:* 1673-1679, 1993. PMID: 7694868.

11 Ma Y, Xu Y, Tang L, Zhang Z, Wang J and Wang H: Cytokine-induced killer (CIK) cell therapy for patients with hepatocellular carcinoma: efficacy and safety. Exp Hematol Oncol *1(1):* 11, 2012. PMID: 23210562. DOI:10.1186/2162-3619-1-11

12 Schmidt-Wolf IGH, Lefterova P, Johnston V, Huhn D, Blume KG and Negrin R: Propagation of large numbers of T-cells with natural killer cell markers. Br J Haematol *87(3):* 453-458, 1994. PMID: 7527643. DOI: 10.1111/j.1365-2141.1994.tb08297.x

13 Cossarizza A, Chang HD, Radbruch A, Akdis M, Andrä I, Annunziato F, Bacher P, Barnaba V, Battistini L, Bauer WM, Baumgart S, Becher B, Beisker W, Berek C, Blanco A, Borsellino G, Boulais PE, Brinkman RR, Büscher M, Busch DH, Bushnell TP, Cao X, Cavani A, Chattopadhyay PK, Cheng Q, Chow S, Clerici M, Cooke A, Cosma A, Cosmi L, Cumano A, Dang VD, Davies D, De Biasi S, Del Zotto G, Della Bella S, Dellabona P, Deniz G, Dessing M, Diefenbach A, Di Santo J, Dieli F, Dolf A, Donnenberg VS, Dörner T, Ehrhardt GRA, Endl E, Engel P, Engelhardt B, Esser C, Everts B, Dreher A, Falk CS, Fehniger TA, Filby A, Fillatreau S, Follo M, Förster I, Foster J, Foulds GA, Frenette PS, Galbraith D, Garbi N, García-Godoy MD, Geginat J, Ghoreschi K, Gibellini L, Goettlinger C, Goodyear CS, Gori A, Grogan J, Gross M, Grützkau A, Grummitt D, Hahn J, Hammer Q, Hauser AE, Haviland DL, Hedley D, Herrera G, Herrmann M, Hiepe F, Holland T, Hombrink P, Houston JP, Hoyer BF, Huang B, Hunter CA, Iannone A, Jäck HM, Jávega B, Jonjic S, Juelke K, Jung S, Kaiser T, Kalina T, Keller B, Khan S, Kienhöfer D, Kroneis T, Kunkel D, Kurts C, Kvistborg P, Lannigan J, Lantz O, Larbi A, LeibundGut-Landmann S, Leipold MD, Levings MK, Litwin V, Liu Y, Lohoff M, Lombardi G, Lopez L, Lovett-Racke A, Lubberts E, Ludewig B, Lugli E, Maecker HT, Martrus G, Matarese G, Maueröder C, McGrath M, McInnes I, Mei HE,

Melchers F, Melzer S, Mielenz D, Mills K, Mirrer D, Mjösberg J, Moore J, Moran B, Moretta A, Moretta L, Mosmann TR, Müller S, Müller W, Münz C, Multhoff G, Munoz LE, Murphy KM, Nakayama T, Nasi M, Neudörfl C, Nolan J, Nourshargh S, O'Connor JE, Ouyang W, Oxenius A, Palankar R, Panse I, Peterson P, Peth C, Petriz J, Philips D, Pickl W, Piconese S, Pinti M, Pockley AG, Podolska MJ, Pucillo C, Quataert SA, Radstake TRDJ, Rajwa B, Rebhahn JA, Recktenwald D, Remmerswaal EBM, Rezvani K, Rico LG, Robinson JP, Romagnani C, Rubartelli A, Ruckert B, Ruland J, Sakaguchi S, Sala-de-Oyanguren F, Samstag Y, Sanderson S, Sawitzki B, Scheffold A, Schiemann M, Schildberg F, Schimisky E, Schmid SA, Schmitt S, Schober K, Schüler T, Schulz AR, Schumacher T, Scotta C, Shankey TV, Shemer A, Simon AK, Spidlen J, Stall AM, Stark R, Stehle C, Stein M, Steinmetz T, Stockinger H, Takahama Y, Tarnok A, Tian Z, Toldi G, Tornack J, Traggiai E, Trotter J, Ulrich H, van der Braber M, van Lier RAW, Veldhoen M, Vento-Asturias S, Vieira P, Voehringer D, Volk HD, von Volkmann K, Waisman A, Walker R, Ward MD, Warnatz K, Warth S, Watson JV, Watzl C, Wegener L, Wiedemann A, Wienands J, Willimsky G, Wing J, Wurst P, Yu L, Yue A, Zhang Q, Zhao Y, Ziegler S and Zimmermann J: Guidelines for the use of flow cytometry and cell sorting in immunological studies. Eur J Immunol *47*: 1584-1797, 2017. PMID: 29023707. DOI: 10.1002/eji.201646632

14 Applied Biosystems: Guide to performing relative quantitation of gene expression using real-time quantitative PCR. Applied Biosystems, pp. 56-59, 2008. Available at: https://assets.thermofisher.com/TFS-Assets/LSG/manual s/cms_042380.pdf [Last accessed June 29, 2020]

15 Epis MR, Giles KM, Candy PA, Webster RJ and Leedman PJ: *miR-331-3p* regulates expression of neuropilin-2 in glioblastoma. J Neurooncol *116:* 67-75, 2014. PMID: 24142150. DOI: 10.1007/s11060-013-1271-7

16 Gao D, Cai Y, Chen Y, Li W, Wei CC, Luo X and Wang Y: Novel TLR7 agonist stimulates activity of CIK/NK immunological effector cells to enhance antitumor cytotoxicity. Oncol Lett *15:* 5105-5110, 2018. PMID: 29552145. DOI: 10.3892/ol.2018.7954

17 Nakayama H, Bruneau S, Kochupurakkal N, Coma S, Briscoe DM and Klagsbrun M: Regulation of mTOR signaling by semaphorin 3F-neuropilin 2 interactions *in vitro* and *in vivo*. Sci Rep *5:* 11789, 2015. PMID: 26156437. DOI: 10.1038/srep11789

18 Zhao JJ, Zhou S, Chen CL, Zhang HX, Zhou ZQ, Wu ZR, Liu Y, Pan QZ, Zhu Q, Tang Y, Xia JC and Weng DS: Clinical effect of adjuvant cytokine-induced killer cells immunotherapy in patients with stage II-IVB nasopharyngeal carcinoma after chemoradiotherapy: A propensity score analysis. J Cancer *9:* 4204-4214, 2018. PMID: 30519321. DOI: 10.7150/jca.25790

19 Meng M, Li L, Li R, Wang W, Chen Y, Xie Y, Han R, Zhu K, Huang W, Yang L, Li S, Shi J, Tan W, Gao H, Zhao Y, Yang L, Tan J and Hou Z: A dynamic transcriptomic atlas of cytokine-induced killer cells. J Biol Chem *293:* 19600-19612, 2018. PMID: 30333226. DOI: 10.1074/jbc.RA118.003280

20 Franceschetti M, Pievani A, Borleri G, Vago L, Fleischhauer K, Golay J and Introna M: Cytokine-induced killer cells are terminally differentiated activated CD8 cytotoxic T-EMRA lymphocytes. Exp Hematol *37:* 616-628.e2, 2009. PMID: 19375652. DOI: 10.1016/j.exphem.2009. 01.010

21 Liu Y, Liu H, Liu H, He P, Li J, Liu X, Chen L, Wang M, Xi J, Wang H, Zhang H, Zhu Y, Zhu W, Ning J, Guo C, Sun C and Zhang M: Dendritic cell-activated cytokine-induced killer cell-mediated immunotherapy is safe and effective for cancer patients >65 years old. Oncol Lett *12:* 5205-5210, 2016. PMID: 28105230. DOI: 10.3892/ol.2016.5337

22 Gao X, Mi Y, Guo N, Xu H, Xu L, Gou X and Jin W: Cytokine-induced killer cells as pharmacological tools for cancer immunotherapy. Front Immunol. *8:* 774, 2017. PMID: 28729866. DOI:10.3389/fimmu.2017.00774

23 Lv T, Wu X, Sun L, Hu Q, Wan Y, Wang L, Zhao Z, Tu X and Xiao ZJ: p53-R273H upregulates neuropilin-2 to promote cell mobility and tumor metastasis. Cell Death Dis *8:* e2995, 2017. PMID: 28796261. DOI: 10.1038/cddis.2017.376

24 Nasarre P, Gemmill RM, Potiron VA, Roche J, Lu X, Barón AE, Korch C, Garrett-Mayer E, Lagana A, Howe PH and Drabkin HA: Neuropilin-2 Is upregulated in lung cancer cells during TGF-β1-induced epithelial–mesenchymal transition. Cancer Res *73:* 7111-7121, 2013. PMID: 24121493. DOI: 10.1158/0008-5472.CAN-13-175

4. Discussion with references

The immunology of tumors includes an area of research and therapy aimed, on the one hand, to investigate the interactions between the immune system and cancer, on the other, to identify and propose therapeutic solutions based on the stimulation of the effector components of the immune system (Yu, S. et al. 2017). In the field of immunotherapy applied to the treatment of tumors there are several therapeutic approaches, but certainly one of the most fascinating is that based on the use of effector cells of the immune system (cellular immunotherapy), armed selectively against cancer cells (Arnaud, M. et al. 2021). Some kinds of immunotherapy are authorized in Europe, in line with the most advanced studies that show how this type of approach can concretely improve the life of some patients, even in the case of childhood cancers (Hayden, P.J. et al. 2022). Cytokine-induced killer cells (CIKs), T cells expanded in vitro and characterized by a potent anti-tumor activity, represent an encouraging immunotherapy strategy in the oncological field (Wang, S. et al. 2020). CIK cells have a significant antitumor activity and are able to eradicate tumors with few side effects. They are a very encouraging cell population with an inexpensive expansion protocol which could yield to superior clinical outcome in clinical trials employing adoptive cellular therapy combination (Cappuzzello, E. et al. 2017). They are a subpopulation of lymphocytes characterized by the expression of CD3$^+$ and CD56$^+$ which are surface markers common to T lymphocytes and natural killer NK cells. They possess a high proliferation rate and potent antitumor effects. CIK cells are capable of exerting a potent MHC-unrestricted cytotoxicity against both hematological and solid tumors, but not hematopoietic precursors and normal tissues (Wang, X, et al. 2014). The use of immune therapy for the treatment of hematological malignancies is an effective obvious treatment, as they are more accessible to effector immune cells. However, one disadvantage for these cancers is that the effector immune cells may potentially be malignant themselves. The differences of the outcomes in different kinds of cancers could result from different molecular mechanisms unexplained yet. The main aim of this study is to investigate the combinatorial effect of CBD and CIK cells, particularly in

pancreatic cancer (PC) and multiple myeloma (MM). Although the expression and function of CB2 receptors has been widely studied in several immune cells, this is the first study reporting a detailed characterization of CB2 receptors expression on distinct CIK cells populations. The factors and conditions that regulate CB2 expression are still poorly understood, and the signaling cascades are incomplete. We have shown that CIK cells on days 7 and 14 of *ex vivo* expansion express remarkable high levels of CB2 receptors compared to PBMCs. We performed polychromatic flow cytometry which revealed also high levels of CB2 receptors expression in MM cell lines. Human pancreatic cancer PC cell lines and tumor biopsies have been also shown previously to express higher levels of cannabinoid receptors compared to normal pancreatic tissue. Further, our study demonstrated that CBD can be protective regarding CIK cells since the LDH release was decreasing in a dose-dependent manner. However, CBD used during CIK cells expansion was able to decrease the percentage of NKT cells, but the percentage of NKG2D-positive NKT cells did not change and remained high. We found that IL-2 primarily determines the expression of CB2 receptor on CIK cells. Moreover, the percentages of CB2 positive cells always remains high, regardless of co-culturing with any CIK cell mediators (anti-CD3 antibody, IFN-γ, IL-2, IL-15, and IL-1β). The cytokine cocktail used for CIK cells expansion includes IL-2 to promote survival and the expression of the natural killer group 2 member D (NKG2D) transmembrane adapter protein DAP10, which in turn is essential for cytolysis, and IL-15, which is capable of further activating CIK cells and shares common signaling components with IL-2, e.g., activation of the Jak/STAT signaling pathways. Previously, it has been shown that CB2 signaling in unstimulated human immunocompetent primary leukocytes (peripheral blood mononuclear cells (PBMCs)) induces the phosphorylation of p38 MAPKs, downstream CREB phosphorylation and induction of IL-6, IL-10 cytokine secretion. Therefore, we also immunophenotyped CIK cells on days 7 and day 14 of *ex vivo* expansion for intracellular p-p38 expression. Interestingly, we found that CIK cells showed a low level of intracellular p-p38, primarily in the subset of T lymphocytes at day 7, whereas it was undetectable in other subsets at either day 7 or day 14.

Similarly, we immunophenotyped PANC-1 pancreatic cancer cell line and observed p-38 undetectable via flow cytometry. In the case of p-CREB, when CIK cells (day 14) were incubated with CBD, we found a weak and variable signal among donors which could be explained with different subtypes of CB2 receptor. The CB2 receptors, GPCRs, once activated are typically internalized and degraded. Alternatively, they are recycled to the membrane for another activation cycle. An independent interesting study has also recently identified the scaffold/phagosomal protein p62/SQSTM1 as part of the CB2 receptor interactome in transiently transfected HEK293 cells mainly in the plasma membrane. Degradation of CB2 receptors can occur via lysosome and autophagy pathways where p62 protein is involved. We also investigated whether CB2 receptors colocalize with p62 vesicles in CIK cells and PANC-1 cells by using immunocytochemical studies and a 3D reconstruction modeling of confocal images. Our analysis clearly showed that p62 vesicles were surrounded by CB2-positive areas at the surface membrane and also intracellularly in CIK cells, while in the case of PANC-1 we used segmentation algorithm and determined that p62-positive regions were co-expressed with CB2. Using multiple methods we investigate whether inducing CIK cells with cannabidiol can enhance their cytotoxicity primarily on MM and PC in this study. The results of the CCK-8 and LDH cytotoxicity assay showed that CBD can affect the viability of PC and MM cells. These results confirm the antitumor potential of CBD against MM and PC, which was already reported by other studies. Interestingly, when CIK cells were co-cultured with MM or PC cells, a concentration-dependent inhibitory response (high concentration) was observed in these cells also via Flow Cytometry analysis. However, CBD (in low concentration) increased the cytotoxicity of CIK cells, which in turn negatively impacted the viability of pancreatic cancer cells. As CIK cell therapy is safe, introducing a low dose of pure cannabidiol particularly for the non-respondent patients may help to stimulate the cytotoxic function of CIK cells and increase the therapeutic response. Finally, we aimed to investigate the expression of Neuropilin proteins, NRP1 and NRP2, both originally discovered as neuronal adhesion molecules, on CIK cells at different stages of maturation. We analyzed

CIK cells at different time points via Flow Cytometry and quantitative real-time polymerase chain reaction qRT-PCR for neuropilins expression. Phenotyping results showed CIK cells having develop properly, and low levels of NRP2 were detected. On the other hand, no NRP1 was found. Recognizing NRP2 in CIK cells might help to improve CIK cells cytotoxicity.

References

E Cappuzzello, R Sommaggio, P Zanovello, A Rosato. Cytokines for the induction of antitumor effectors: The paradigm of Cytokine-Induced Killer (CIK) cells. Cytokine Growth Factor Rev. 2017.

M Arnaud, S Bobisse, J Chiffelle, A Harari. The Promise of Personalized TCR-Based Cellular Immunotherapy for Cancer Patients. Front Immunol. 2021.

P J Hayden, C Roddie, P Bader, G W Basak, H Bonig, C Bonini, C Chabannon, F Ciceri, S Corbacioglu, R Ellard, F Sanchez-Guijo, U Jäger, M Hildebrandt, M Hudecek, MJ Kersten, U Köhl, J Kuball, S Mielke, M Mohty, J Murray, A Nagler, J Rees, C Rioufol, R Saccardi, J A Snowden, J Styczynski, M Subklewe, C Thieblemont, M Topp, Á U Ispizua, D Chen, R Vrhovac, J G Gribben, N Kröger, H Einsele, I Yakoub-Agha. Management of adults and children receiving CAR T-cell therapy: 2021 best practice recommendations of the European Society for Blood and Marrow Transplantation (EBMT) and the Joint Accreditation Committee of ISCT and EBMT (JACIE) and the European Haematology Association (EHA). Ann Oncol. 2022.

S Wang, X Wang, X Zhou, H K Lyerly, M A Morse and J Ren. DC-CIK as a widely applicable cancer immunotherapy. Expert Opinion on Biological Therapy. 2020.

S Yu, A Li, Q Liu, T Li, X Yuan, X Han, K Wu. Chimeric antigen receptor T cells: A novel therapy for solid tumors. J. Hematol. Oncol. 2017.

X Wang, W Yu, H Li, J Yu, X Zhang, X Ren, S Cao. Can the dual-functional capability of CIK cells be used to improve antitumor effects?. Cell Immunol. 2014.

5. Acknowledgement

This work was performed at the Department of Integrated Oncology under the supervision of Prof. Dr. med Ingo Schmidt-Wolf, at the University Hospital of Bonn, Rheinische Friedrich-Wilhelms-Universität Bonn, Bonn, Germany.

Especially, I would like to thank Prof. Schmidt-Wolf for giving me the possibility to work on my doctoral thesis and for his guidance and support supervising my doctoral thesis and for his advice, encouragement during my doctoral work progress.

Specifically, I would like to thank my second supervisor Prof. Dr. Hinrich Abken for his support and review of this thesis. I want to thank Prof. Dr. Christian Kurts and PD Dr. Maria Carmona-Gonzalez for being part of my dissertation committee.

Moreover, I would like to thank all members of the research laboratory at the Department of Integrated Oncology for their support and encouragement.

Finally, I would like to thank all members of my family and friends for their support and patience during my doctoral work.